Boumaiza, L., Stotler, R.L., Mayer, B., Matiatos, I., Sacchi, E., Otero, N., Johannesson, K.H., Huneau, F., Chesnaux, R., Blarasin, M., Re, V., **Knöller, K.** (2024):
How the $\delta^{18}O_{NO3}$ versus $\delta^{15}N_{NO3}$ plot can be used to identify a typical expected isotopic range of denitrification for NO_3-impacted groundwaters
ACS ES&T Wat. **4** (12), 5243 - 5254

How the $\delta^{18}O_{NO3}$ versus $\delta^{15}N_{NO3}$ plot can be used to identify a typical expected isotopic range of denitrification for NO_3-impacted groundwaters

Lamine Boumaiza[1*], Randy L. Stotler[2], Bernhard Mayer[3], Ioannis Matiatos[4], Elisa Sacchi[5], Neus Otero[6,7], Karen H. Johannesson[8], Frédéric Huneau[9], Romain Chesnaux[10], Mónica Blarasin[11], Viviana Re[12], Kay Knöller[13,14]

[1] University of Texas at Austin, Department of Earth and Planetary Sciences, Jackson School of Geosciences, Austin, Texas, 78712, USA,

[2] University of Waterloo, Department of Earth and Environmental Sciences, Waterloo, Ontario, N2L 3G1, Canada

[3] University of Calgary, Department of Earth, Energy and Environment, Calgary, Alberta, T2N 1N4 Canada

[4] Institute of Marine Biological Resources and Inland Waters, Hellenic Centre for Marine Research, Anavissos Attikis, 19013, Greece

[5] University of Pavia, Department of Earth and Environmental Sciences, Interdepartmental Centre for Water Research, Pavia, 27100, Italy

[6] Universitat de Barcelona, Departament de Mineralogia, Petrologia i Geologia Aplicada, Barcelona, 08028, Spain

[7] Universitat de Barcelona, Institut de Recerca de l'Aigua, Barcelona, 08028, Spain

[8] University of Massachusetts Boston, School for the Environment, Boston, Massachusetts, 02125, USA

[9] Université de Corse, CNRS UMR 6134 SPE, Département d'Hydrogéologie, Corte, 20250, France

[10] Université du Québec à Chicoutimi, Département des Sciences Appliquées, Saguenay, Québec, G7H 2B1, Canada

[11] Universidad Nacional de Río Cuarto, Departamento de Geología, Río Cuarto, Córdoba, X5804BYA, Argentina

[12] University of Pisa, Department of Earth Sciences, Pisa, 56126, Italy

[13] Helmholtz Centre for Environmental Research, Department of Catchment Hydrology, Halle, Saale, 06120, Germany

[14] Technical University of Darmstadt, Institute of Applied Geosciences, Darmstadt, 64287, Germany

* *Corresponding Author:* Lamine Boumaiza (lamine.boumaiza@jsg.utexas.edu)

How the $\delta^{18}O_{NO3}$ versus $\delta^{15}N_{NO3}$ plot can be used to identify a typical expected isotopic range of denitrification for NO_3-impacted groundwaters

Abstract

Stable isotope values $\delta^{15}N_{NO3}$ and $\delta^{18}O_{NO3}$ of dissolved nitrate (NO_3) are commonly used to identify the occurrence of denitrification as there is a progressive increase of $\delta^{15}N_{NO3}$ and $\delta^{18}O_{NO3}$ values accompanied by a decrease in NO_3 concentration. Thus, denitrification results in a positive trendline on the dual plot of $\delta^{18}O_{NO3}$ versus $\delta^{15}N_{NO3}$. The combination of two trendlines with different slopes provides the "typical expected isotopic range of denitrification (TEIRD)" on the $\delta^{18}O_{NO3}$ versus $\delta^{15}N_{NO3}$ plot. Many studies distinguished denitrified groundwaters by applying the TEIRD concept that is incorrectly introduced because it assumes a single NO_3 source even though multiple NO_3 sources exist. Also, most TEIRD applications rely on specific denitrification slopes although these are known to vary owing to aquifer changing biogeochemical conditions. Alternatively, an accurate delineation of the TEIRD requires the identification of all potential NO_3 sources in the aquifer with their measured or reconstructed $\delta^{15}N_{NO3}$ and $\delta^{18}O_{NO3}$ values. This allows then for an accurate TEIRD to be traced with two denitrification trendlines having a slope corresponding to that from the correlation of the measured $\delta^{18}O_{NO3}$ and $\delta^{15}N_{NO3}$ values. Ultimately, each NO_3 source can have a specific TEIRD, although denitrification trendlines for multiple NO_3 sources can feature the same slope within a single aquifer.

Keywords

Nitrate, Groundwater, Reconstructed $\delta^{15}N_{NO3}$, Reconstructed $\delta^{18}O_{NO3}$, Isotope fractionation.

1 Introduction

The growth of human population concomitant with intensive use of manure and industrial fertilizers in agricultural lands, disposal of municipal/septic wastewater, and fossil fuel combustion caused a tremendous increase of reactive nitrogen (N) loadings to hydrosystems worldwide [1–3]. In groundwater systems, the most common nitrogenous contaminant is nitrate (NO_3), which is recognized to contribute groundwater quality deterioration. Mitigating NO_3 groundwater contamination requires identifying potential sources of NO_3, estimating their relative contributions, tracing NO_3 dispersal distribution, and recognizing potential subsurface biogeochemical transformation processes controlling the NO_3 evolution within groundwater systems [4–7]. This investigation process remains challenging due to the coexistence often of multiple NO_3 sources governed by various biogeochemical N-cycling processes, such as nitrification, denitrification, and ammonification [8–15]. Dissimilatory NO_3 reduction to ammonium is a two-step process that first reduces NO_3 to nitrite (NO_2) and then to NH_4 ($NO_3 \rightarrow NO_2 \rightarrow NH_4$) [16]. Denitrification is a multi-step process that converts NO_3 to NO_2 and then to unreactive N_2 or other N-containing gases ($NO_3 \rightarrow NO_2 \rightarrow N_2/N_2O/NO$). Ammonification is a microbial-driven process of N-organic decomposition resulting in the release of ammonium (NH_4) in the environment that usually undergoes rapid nitrification to nitrate under oxic conditions [16]. Although these processes serve different functions in the N-cycle, they impact the isotopic composition of residual NO_3 in groundwater systems [17]. Therefore, the naturally occurring stable isotope ratios of N ($^{15}N/^{14}N$) and O ($^{18}O/^{16}O$) in NO_3, commonly expressed in delta (δ) per mil (‰) notation as $\delta^{15}N_{NO3}$ and $\delta^{18}O_{NO3}$ (hereafter referred to as NO_3-isotope composition), provides an invaluable and effective tool that can be used to infer the predominant subsurface N transformation processes in groundwater systems [18,19].

Studies investigating the behavior of NO_3-isotope compositions in groundwater, with decreasing NO_3 concentrations due to reduction from denitrification, observed a progressive increase of $\delta^{18}O_{NO3}$ and $\delta^{15}N_{NO3}$ values in the remaining NO_3 pool. Earlier studies identified correlations with straight trends having slopes of 0.5 to 0.8 on the $\delta^{18}O_{NO3}$ versus $\delta^{15}N_{NO3}$ plot [20–22]. This salient trend has long been considered as a unique diagnostic response of denitrification [19,23], assuming a constrained

isotope fractionation effect during enzymatic bond-breakage [24–26], whereas the effect of isotopic fractionation due to ammonification is poorly understood [27]. Further, by using the advent of the denitrifier analytical method [28,29], the proportionality of isotopic fractionation associated with NO_3 reduction in terrestrial ecosystems was observed to follow a larger range of slopes (i.e., 0.5-2) than observed in earlier studies (i.e., 0.5-0.8) [20,21,30–32], whereas in marine ecosystems the slope has a narrower range of 0.9-1 [33–36]. Changes in dissolved oxygen (DO), mixing of multiple NO_3 sources, salinity, pH, microbial cultures, organic matter content and geological characteristics are the main parameters controlling the observed differences between marine and terrestrial ecosystems [18,19,37–39].

2 General concern

Böttcher et al.[20] investigated the denitrification process through a set of groundwater samples (Figure SF1a), for which they found that in the $\delta^{18}O_{NO3}$ versus $\delta^{15}N_{NO3}$ plot, the values display a positive correlation with a straight line having a slope of 0.48 (i.e., 1/2.1). This indicates that $\delta^{15}N_{NO3}$ values shift 2.1 times more than $\delta^{18}O_{NO3}$ (this shift is referred in this manuscript to as “lambda” (Λ)[40]). Fukada et al. [41] also investigated the occurrence of denitrification in a groundwater system (Figure SF1b) and identified a positive correlation between $\delta^{18}O_{NO3}$ and $\delta^{15}N_{NO3}$ values of the remaining NO_3 with a slope of 0.76 (i.e., 1/1.3) indicating an increase of $\delta^{15}N_{NO3}$ compared to $\delta^{18}O_{NO3}$ values with Λ of 1.3. Other field studies reported different Λ values such as 1 [19], 1.4 [30], 1.7 [32], 1.8 [42], and 2.2 [43]. Although the observed difference in Λ values is consistent with the fact that isotopic fractionation is dependent on local physico-chemical conditions (e.g., redox conditions), microbial community, and land use/cover of each site [19,43], several groundwater studies relied further on these Λ values to justify the occurrence of microbial denitrification [44–46]. Subsequently, combining two sloped straight lines representing two different Λ values became a common practice to delineate —on the dual $\delta^{18}O_{NO3}$ versus $\delta^{15}N_{NO3}$ plot— the range of potential denitrification. In the literature, this has been termed using a variety of nomenclatures including "ideal zone for denitrification" [47], "typical upper and lower slope boundaries for denitrification" [48], and "range of denitrification" [49]. In this manuscript, this is called the "typical expected isotopic range of denitrification (TEIRD)".

There are two combinations of two sloped straight lines (i.e., TEIRD) that are most commonly used in the literature. The first combination includes the Λ values for denitrification proposed by Böttcher et al.[20] and Fukada et al. [41], whereby the TEIRD is constrained by two trends with slopes of 0.48 and 0.76, respectively (referred hereafter as 0.48/0.76-TEIRD). For example, Ding et al. [50] assessed denitrification in groundwater from the aquifer system of the Hohhot Basin (China), in which they assumed the occurrence of denitrification in groundwater samples that plot within the 0.48/0.76-TEIRD (Figure SF1c). The second combination consists of a larger TEIRD constrained by two sloped straight lines corresponding (i) to an increase of $\delta^{15}N_{NO3}$ by a Λ value of 2 compared to $\delta^{18}O_{NO3}$ (slope of 0.5, i.e., 1/2), and (ii) an equal increase of $\delta^{15}N_{NO3}$ against $\delta^{18}O_{NO3}$ values involving a Λ value of 1 (slope of 1, i.e., 1/1). This second TEIRD is referred to hereafter as 0.5/1-TEIRD. An example of the application of the 0.5/1-TEIRD is shown in Figure SF1d, through which Zaryab et al. [51] investigated NO_3 sources and fate in the Kabul Plain aquifer (Afghanistan).

It is important to mention that TEIRD includes groundwater samples with measured $\delta^{15}N_{NO3}$ and $\delta^{18}O_{NO3}$ values different to that of the original NO_3 source because the NO_3-isotope composition is expected to be modified due to partial removal of NO_3 by denitrification. However, this change of NO_3-isotope composition may not always be indicative of denitrification because NO_3 in the pool can be simultaneously supplied by other NO_3 sources as some NO_3 is removed via denitrification [19,52]. Hence, an accurate TEIRD definition for tracking the denitrification process requires that the initial $\delta^{15}N_{NO3}$ [i.e., $(\delta^{15}N_{NO3})_0$] and initial $\delta^{18}O_{NO3}$ [i.e., $(\delta^{18}O_{NO3})_0$] values of the NO_3 source be determined. Nonetheless, this prerequisite information is commonly neglected in field studies, such that the original concept regarding the TEIRD is applied with uncertain knowledge of the $(\delta^{15}N_{NO3})_0$ and $(\delta^{18}O_{NO3})_0$ values in the groundwater pool. Therefore, the main objective of this paper is to investigate the common shortcomings of the application of the TEIRD concept by examining a variety of case studies. From this examination, an approach is proposed for delineating the TEIRD on the $\delta^{18}O_{NO3}$ versus $\delta^{15}N_{NO3}$ plot leading to less potential uncertainties on an assumed denitrified groundwater.

3 Specific concern on the typical expected isotopic range of denitrification

While the combination of two straight lines with different slopes (e.g., 0.5/1-TEIRD) is commonly used for defining the TEIRD on the $\delta^{18}O_{NO3}$ versus $\delta^{15}N_{NO3}$ plot, other researchers have constrained the TEIRD with two parallel lines having identical slopes. An example of this application is shown in Figure SF1e, wherein Mayer et al. [23] indicated that both straight lines correspond to microbial denitrification under similar conditions assuming that the NO_3-isotope composition was derived from nitrification in soils. Martinelli et al. [53] also constrained the TEIRD with two straight lines having identical slopes of 0.5 but corresponding to two different sources, i.e., one line represents higher $\delta^{18}O_{NO3}$ values originating from mineralized fertilizers with $\delta^{15}N_{NO3}$ values near to 0‰, whereas the second line represents lower $\delta^{18}O_{NO3}$ values originating from manure and septic system effluents with more elevated $\delta^{15}N_{NO3}$ values (Figure SF1f). Interestingly, these two examples specified that denitrification occurred for initial NO_3 originating from different sources (e.g., mineralized fertilizers and manure/septic system effluents; Figure SF1f). However, the initial $(\delta^{15}N_{NO3})_0$ and $(\delta^{18}O_{NO3})_0$ values corresponding to each NO_3 source were not specified. This is important because denitrification originating from one specific NO_3-zone, without specifying the values of $(\delta^{15}N_{NO3})_0$ and $(\delta^{18}O_{NO3})_0$, can be illustrated by several different denitrification trends (see an example from Figure SF1e, in which two denitrification trends originate from the same NO_3-zone, i.e., NO_3 derived from nitrification in soils) leading to potential biased interpretation of denitrified groundwaters.

Other studies applied the 0.48/0.76-TEIRD or 0.5/1-TEIRD concepts with two sloped lines that intersect at a specific point. These studies include Wang et al. [54] who investigated NO_3 in water with 0.5/1-TEIRD originating from a source that had $\delta^{15}N_{NO3}$ and $\delta^{18}O_{NO3}$ values corresponding to the lower NO_3-isotope endmembers of the manure/sewage zone (Figure SF1g). Torres-Martínez et al. [47] used 0.48/0.76-TEIRD originating from a point having a $\delta^{15}N_{NO3}$ value of +5‰ and a $\delta^{18}O_{NO3}$ value of −5‰ (Figure SF1h). Both studies did not state how the point where the two sloped lines intersect was determined or what assumptions led to the proposed values of $\delta^{15}N_{NO3}$ and $\delta^{18}O_{NO3}$ corresponding to these points.

A field-based study that traced TEIRD using isotope compositions of the sources of NO_3 was undertaken by Lorette et al. [55], who sampled primary sources of NO_3 including agricultural soils and sewage to investigate the impact of the addition of synthetic fertilizers on the Toulon catchment system in France. Lorette et al. [55] considered two TEIRDs for the same investigated area, namely one TEIRD for NO_3 derived from the assessed cultivated soil endmembers and another TEIRD for NO_3 derived from the assessed sewage endmembers. Both TEIRDs are constrained with two parallel straight lines having identical slopes of 0.5 as shown in Figure SF1i, in which the measured $\delta^{15}N_{NO3}$ and $\delta^{18}O_{NO3}$ values in groundwater samples were consistent with a N-soil source with denitrification causing a deviation of the initial isotopic signature of the NO_3 source [55]. This approach of delineating the TEIRD is interesting because it is based, first, on deriving representative field-based initial NO_3 isotopic composition of the NO_3 source, and second, using the derived values to trace the TEIRD. However, the traced TEIRD employed slopes from the literature (i.e., 2:1, i.e., 0.5, Figure SF1i), rather than the actual denitrification slope shown by samples from the investigated aquifer system.

Several studies defined the TEIRD by integrating a single NO_3 source with a single initial NO_3 isotopic composition, from which two theorical denitrification trends are traced (e.g., from Figure SF1c-d). Although most studies have not cited the reference of the adopted theoretical TEIRD concept, it appears in many cases to be that from Kendall et al. [19] (Figure 1) as indicated by Ye et al. [56]. Here, it is important to mention that Kendall et al. [19] did not indicate that this concept concerns TEIRD, rather, the two trends in Figure 1 are examples corresponding to two separate typical expected slopes for data resulting from denitrification of a single NO_3 source having a $\delta^{15}N_{NO3}$ value of +6‰ and a $\delta^{18}O_{NO3}$ value of −9‰ [19]. The intention of Kendall et al. [19] was not to suggest that both sloped trendlines are valid for the same aquifer and could form a TEIRD originating from a single point where the trendlines intersect (*pers. commun. with Carol Kendall, 2024*). Hence, it appears that the concept of TEIRD was —unintentionally— incorrectly applied by some researchers, involving potential uncertainties regarding an assumed denitrified groundwater. Although several studies were likely not intending to define a TEIRD, meaning that two sloped trendlines were introduced as indicative of potential expected

denitrification trends, most studies did consider a single initial NO_3 isotopic composition for the whole NO_3 pool, even though multiple NO_3 sources exist [48,57–59]. This can lead to uncertainties regarding where denitrified-groundwaters plot within the assumed TEIRD. In the subsequent section, some of the available approaches for determining the initial $(\delta^{15}N_{NO3})_0$ and $(\delta^{18}O_{NO3})_0$ values (i.e., the reconstructed $(\delta^{15}N_{NO3})_0$ and $(\delta^{18}O_{NO3})_0$ values) are introduced and evaluated with available data from case studies. This is introduced for evaluating whether the correlation of reconstructed $(\delta^{15}N_{NO3})_0$ and/or $(\delta^{18}O_{NO3})_0$ values, for a set of groundwater samples belonging to same study area, plot at a single location where two sloped denitrification trendlines intersect (i.e., origin of the TEIRD).

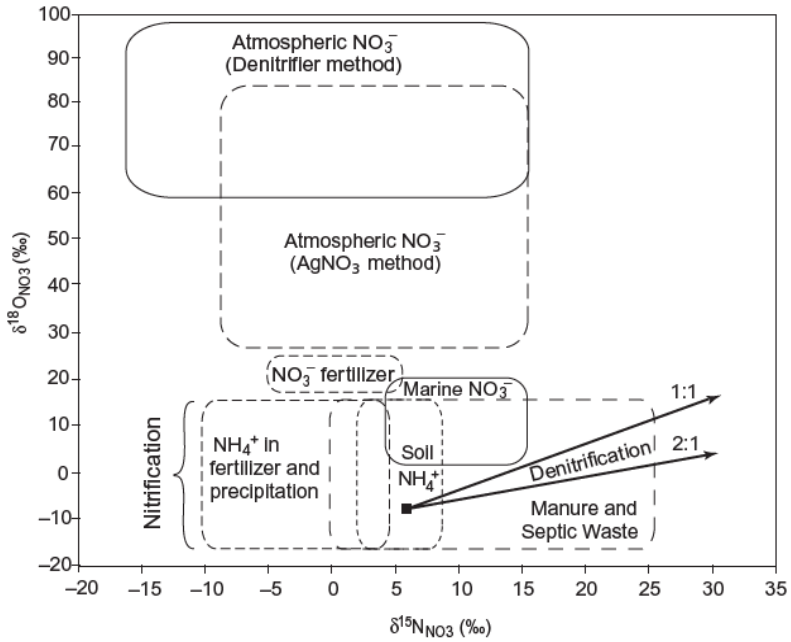

Figure 1. Kendall diagram with example of two trends (i.e., 1:1 and 2:1) indicating two potential separate typical expected slopes for data resulting from denitrification of a NO_3 source having $\delta^{15}N_{NO3}$ value of +6‰ and $\delta^{18}O_{NO3}$ value of −9‰ (this Figure 1 is adapted from Kendall et al. [19]. Copyright 2008 with permission of John Wiley and Sons Inc.)

4 Available approaches for reconstructing the initial NO_3-isotope composition

4.1 Heaton et al. (1983) model

Heaton et al. [60] proposed a model for reconstructing the $(\delta^{15}N_{NO3})_0$ value in groundwater where denitrification has occurred by using Equation 1, in which $(\delta^{15}N_{NO3})_0$ is the initial $\delta^{15}N_{NO3}$ value (‰); $\delta^{15}N_{N2}$ is the measured isotopic value (‰) of the di-nitrogen (N_2; expressed by ml_n/L); N_{2WEA} is a

constant of 9.97 ml_n/L corresponding to the concentration of N_2 under equilibrium with the atmosphere at 22 °C; $\delta^{15}N_{NO3}$ is the measured N isotope ratio of NO_3 (‰); NO_3 is the measured concentration of NO_3 (meq/L); and $(NO_3)_0$ is the initial NO_3 concentration (meq/L).

$$(\delta^{15}N_{NO3})_0 = [0.0893\ (\delta^{15}N_{N2} \times N_2 - 0.7\ N_{2WEA}) + \delta^{15}N_{NO3} \times NO_3] / (NO_3)_0 \quad (1)$$

Whereas the above parameters require analytical measurements, except N_{2WEA}, the $(NO_3)_0$ can be assessed according to Equation 2, in which EA is the amount of excess air (ml_n/L). This in turn can be evaluated using Equation 3, in which Ar and He are the measured concentrations (ml_n/L) of radiogenic argon and helium, respectively, and Ar_{WEA} is a constant of 0.26 ml_n/L corresponding to the concentration of Ar in water under equilibrium with the atmosphere.

$$(NO_3)_0 = NO_3 + 0.0893\ (N_2 - N_{2WEA} - 0.781\ EA) \quad (2)$$

$$EA = (Ar - Ar_{WEA} - 0.14\ He) / 0.00934 \quad (3)$$

The Heaton et al. [60] model did not include an approach for reconstructing the $(\delta^{18}O_{NO3})_0$ value. However, the Heaton et al. [60] model does include an equation that can be used to compute the concentrations of $(NO_3)_0$, which is crucial for other NO_3-groundwater features such as the calculation of the isotopic enrichment factor (ε) [61] or determining NO_3 background concentrations without anthropogenic input, which are commonly assumed to range between 5-7 mg/L [62,63]. For evaluating the outcomes of the Heaton et al. [60] model, measured NO_3 concentrations and $\delta^{15}N_{NO3}$ values in groundwater with the reconstructed $(\delta^{15}N_{NO3})_0$ values (Table ST1) are compiled from Heaton et al. [60], who studied NO_3 in groundwater of the Stampriel-Auob aquifer (South Africa). The plot of the measured $\delta^{15}N_{NO3}$ values in groundwater samples versus their measured NO_3 concentrations (Figure 2a) shows a gradual increase of $\delta^{15}N_{NO3}$ values correlated with a decrease of NO_3 concentration in groundwater (R^2 = 0.8), suggesting the potential effect of denitrification [19]. The reconstructed $(\delta^{15}N_{NO3})_0$ values range from +4.4 to +7.2‰, which are consistent with NO_3 being derived from leaching of NO_3 formed by organic decomposition processes in the soil of the recharge area [60]. Although NO_3 groundwater contamination is originating from one source, the reconstructed $(\delta^{15}N_{NO3})_0$

values are not identical, supporting a potential range of $\delta^{15}N_{NO3}$ values for a single NO_3 source, consistent with observation from field data by Lorette et al. [55].

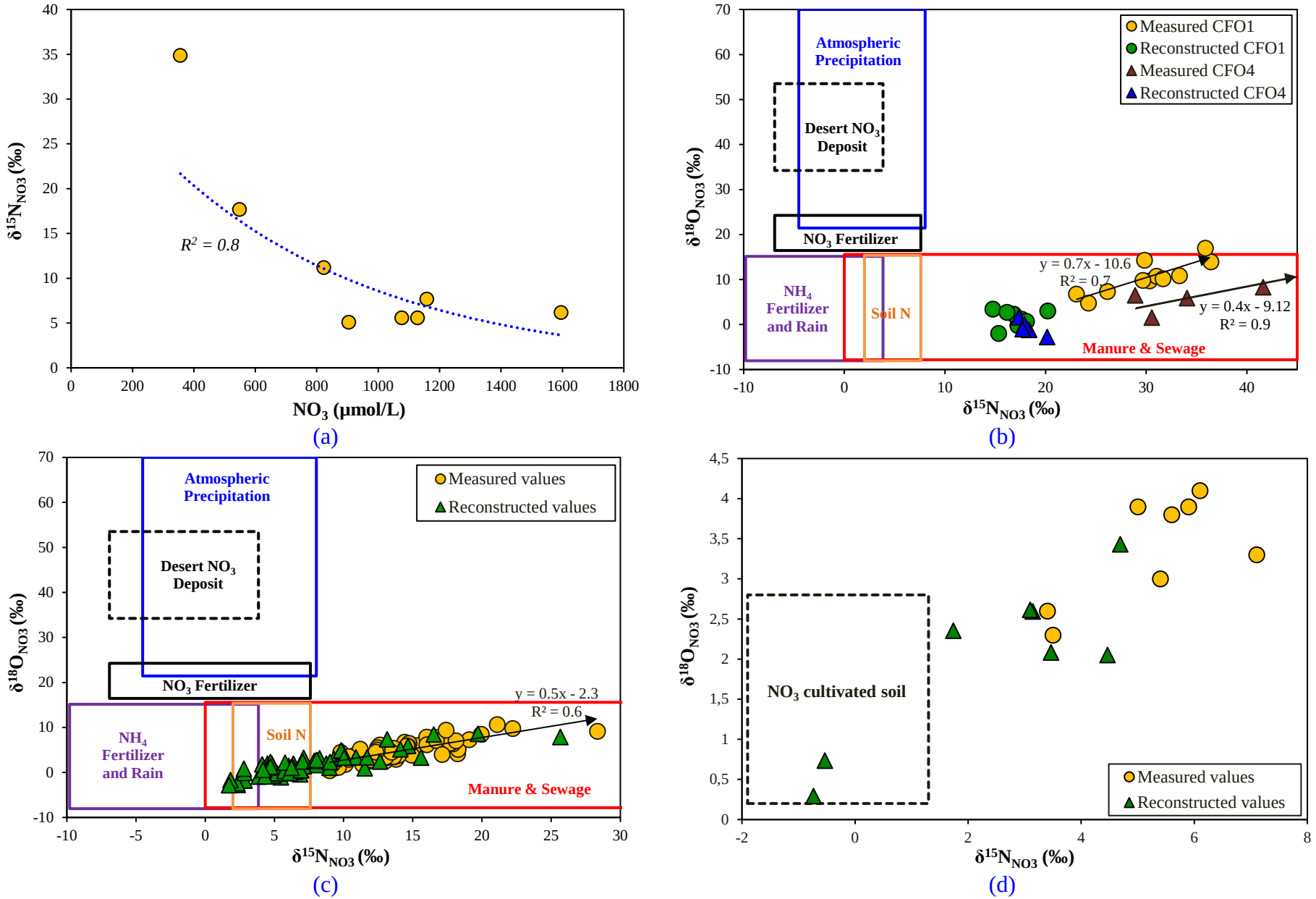

Figure 2. (a) Correlation of measured $\delta^{15}N_{NO3}$ values with measured NO_3 concentrations for groundwater samples from Heaton et al. [60]; (b) Correlation of measured/reconstructed $\delta^{18}O_{NO3}$ versus $\delta^{15}N_{NO3}$ values for groundwater samples from Bourke et al. [64]; (c) Correlation of measured/reconstructed $\delta^{18}O_{NO3}$ versus $\delta^{15}N_{NO3}$ values for groundwater samples from Otero et al. [65]; (d) Correlation of measured/reconstructed $\delta^{18}O_{NO3}$ versus $\delta^{15}N_{NO3}$ values for groundwater samples from Lorette et al. [55]. The endmember values of the boxes in (b) and (c) are from Kendall [66] and Mayer et al. [23]. The reconstructed values in (b) are obtained by a modeling approach, whereas in (c) and (d) are calculated by using a Rayleigh model-based approach.

4.2 **Böhlke et al. (2002) model**

Böhlke et al. [67] used another model for reconstructing the $(\delta^{15}N_{NO3})_0$ by combining data for reactant NO_3 and product excess N_2 gas in denitrified groundwater samples (i.e., excess N_2 gas is believed to be the only product of denitrification). For this simplified model (Equation 4), the concentration of excess N_2 formed by denitrification is estimated from the N_2 and Ar concentrations in groundwater, whereas $(NO_3)_0$ can be determined using Equation 5.

$$(\delta^{15}N_{NO3})_0 = [2(\text{excess } N_2) \times \delta^{15}N_{(\text{excess } N2)} + \delta^{15}N_{NO3} \times NO_3] / (NO_3)_0 \quad (4)$$

$$(NO_3)_0 = NO_3 + 2(\text{excess } N_2) \quad (5)$$

Green et al. [52] used the Böhlke et al. [67] model for reconstructing $(\delta^{15}N_{NO3})_0$ in groundwater from four agricultural watersheds located in California (CA), Nebraska (NE), Washington (WA), and Maryland (MD). They observed a trend of increased reconstructed $(\delta^{15}N_{NO3})_0$ values with age (Figure SF1j), reflecting increased denitrification at locations with older groundwater that likely results from longer reaction times associated with more reduced groundwater [52]. The range of the reconstructed $(\delta^{15}N_{NO3})_0$ values (Figure SF1j) is consistent with a NO_3 source from soil-N or mineral fertilizers, that typically produce $\delta^{15}N_{NO3}$ values varying from −2 to +8‰ [68,69], whereas higher observed $(\delta^{15}N_{NO3})_0$ values >10‰ were associated with a manure source. At the CA site, multiple NO_3 sources were observed having varied $(\delta^{15}N_{NO3})_0$ values with age (Figure SF1j), consistent with a shift from manure to a mineral fertilizer source over time (i.e., 40 year period, Figure SF1j). This finding is explained by the increasing use of mineral fertilizers following the cessation of chicken manure applications at the site [52]. Although the early years at the CA site were dominated by the use of manure, the model of Böhlke et al. [67] indicates that this source then (over the early 10 years) exhibited a range of $\delta^{15}N_{NO3}$ values rather than a single value (Figure SF1j). Dating NO_3-impacted groundwater within the same site is advantageous for better describing when a given NO_3 source started to influence groundwater and determining potential mixing of various NO_3 sources over time.

4.3 **Theoretical $(\delta^{18}O_{NO3})_0$ model**

An approach for reconstructing $(\delta^{18}O_{NO3})_0$ involves estimating a theoretical $(\delta^{18}O_{NO3})_0$ value assuming that all initial NO_3 is derived from nitrification. This approach employs Equation 6 [66], in which $\delta^{18}O_{NO3\ (theoretical)}$ represents the $\delta^{18}O_{NO3}$ prior to isotope fractionation effects due to denitrification (i.e., $(\delta^{18}O_{NO3})_0$). In Equation 6, $\delta^{18}O_{H2O}$ represents the measured stable oxygen isotope ratio in the groundwater sample, whereas $\delta^{18}O_{O2}$ is the isotopic ratio of atmospheric oxygen being a constant value of +23.5‰[70].

$$\delta^{18}O_{NO3\ (theoretical)} = \left(\frac{2}{3}\ \delta^{18}O_{H2O}\right) + \left(\frac{1}{3}\ \delta^{18}O_{O2}\right) \quad (6)$$

Equation 6 is tested with measured and theoretical $\delta^{18}O_{NO3}$ values for groundwater samples (Table ST2) compiled from Boumaiza et al. [15], who studied groundwater NO_3 in the coastal Mediterranean agricultural plain of Oussja-Ghar-Melah, Tunisia. These data indicate that the measured $\delta^{18}O_{NO3}$ values are greater than the reconstructed $(\delta^{18}O_{NO3})_0$ values (i.e., $\delta^{18}O_{NO3\ (theoretical)}$), which is consistent with enrichment of $^{18}O_{NO3}$ possibly due to denitrification occurring in the studied groundwater system. Indeed, Boumaiza et al. [15] observed a positive correlation between the measured $\delta^{18}O_{NO3}$ and $\delta^{15}N_{NO3}$ values with a slope of 0.9. However, the extent of $^{18}O_{NO3}$ enrichment is variable across the sampling locations (Table ST2) suggesting that each sampling site has specific denitrification conditions, consistent with the fact that isotopic enrichment is dependent on local hydrogeochemical conditions. As there is one predominant source of NO_3 for the Oussja-Ghar-Melah groundwater system of (i.e., manure: based on $\delta^{11}B$ values [15]), the reconstructed $(\delta^{18}O_{NO3})_0$ values, which range from +4.0 to +5.1‰, support the concept that the single NO_3 source is characterized by a range of $\delta^{15}N_{NO3}$ and $\delta^{18}O_{NO3}$ values. Hence, data from the Oussja-Ghar-Melah system do not support a TEIRD originating from a single point.

4.4 **Bourke et al. (2019) model**

Bourke et al. [64] used a numerical model for reconstructing both the $(\delta^{15}N_{NO3})_0$ and $(\delta^{18}O_{NO3})_0$ values with a framework of a Monte Carlo modeling approach. More detail on this framework is available

in Bourke et al. [64]. This numerical model was used to investigate the fate of NO_3 in groundwater beneath two separate agricultural areas (i.e., CFO1 and CFO4) in Alberta (Canada), where the application of livestock manure is well documented [64]. The measured and reconstructed $\delta^{15}N_{NO3}$ and $\delta^{18}O_{NO3}$ values for these groundwater samples (Table ST3) are indeed consistent with values for NO_3 derived from manure (Figure 2b). However, although NO_3 contamination is originated from one NO_3 source (i.e., livestock manure), the reconstructed $(\delta^{15}N_{NO3})_0$ and $(\delta^{18}O_{NO3})_0$ values for each site do not plot on a single point (Figure 2b). Hence, the data for these sites in Alberta also support the outcomes from the Heaton et al. [60] and Böhlke et al. [67] models indicating that a single NO_3 source is characterized by a range of $\delta^{15}N_{NO3}$ and $\delta^{18}O_{NO3}$ values rather than one value. The plot of the measured $\delta^{18}O_{NO3}$ versus $\delta^{15}N_{NO3}$ values from both sites shows evidence of denitrified groundwaters, although the denitrification slope within groundwaters from the CFO4 site (slope = 0.4) is lower compared to that from site CFO1 (slope = 0.7) (Figure 2b).

4.5 **Rayleigh model-based approach**

The reconstruction of $(\delta^{15}N_{NO3})_0$ and $(\delta^{18}O_{NO3})_0$ in groundwater systems can be undertaken with Equation 7 (derived from Mariotti et al. [61]), which is introduced here only for $\delta^{15}N_{NO3}$. Note, identical calculations can be applied to reconstruct $(\delta^{18}O_{NO3})_0$. In Equation 7, $\delta^{15}N_{NO3}$ is the measured $\delta^{15}N_{NO3}$ value in groundwater, whereas ε_{15N} is the N isotopic enrichment factor corresponding to the slope from a Rayleigh model that correlates $ln(NO_3/(NO_3)_0)$ with the measured $\delta^{15}N_{NO3}$ values in groundwaters [65]. Whereas the NO_3 value is the measured NO_3 concentration in groundwater, the $(NO_3)_0$ refers to the groundwater natural baseline NO_3 concentration commonly assumed to be in the range of 5-7 mg/L [62,63].

$$(\delta^{15}N_{NO3})_0 = (\delta^{15}N_{NO3}) - \left[\varepsilon_{15N} \cdot \ln\left(\frac{NO_3}{(NO_3)_0}\right)\right] \quad (7)$$

Data from Otero et al. [65] are employed here to evaluate the Rayleigh model-based approach. These data (Table ST4) include NO_3 concentrations and $\delta^{15}N_{NO3}$ and $\delta^{18}O_{NO3}$ values

measured in groundwater samples collected across one field zone (i.e., zone 3) of the Osona aquifer (Spain). The Osona groundwater system is affected by elevated NO_3 concentrations resulting from intensive farming activities based on manure as the primary organic fertilizer with synthetic fertilizers applied only in the areas surrounding villages because the use of manure close to urban areas is forbidden. Potential NO_3 contributions from human wastewater are low as most of the urban settlements are connected to sewage treatment plants [65]. Application of the Rayleigh model using $\delta^{15}N_{NO3}$ and $\delta^{18}O_{NO3}$ values with a theoretical $(NO_3)_0$ concentration of 5 mg/L results in $\varepsilon^{15}N$ and $\varepsilon^{18}O$ values of 2.1 and 1.0‰, respectively, which are subsequently used to reconstruct $(\delta^{15}N_{NO3})_0$ and $(\delta^{18}O_{NO3})_0$ values according to Equation 7. The correlation between the measured $\delta^{18}O_{NO3}$ versus $\delta^{15}N_{NO3}$ values in groundwaters shows a positive trendline with a slope of 0.5 (Figure 2c), suggesting denitrification is occurring within the investigated aquifer zone. The plot of the reconstructed $(\delta^{18}O_{NO3})_0$ versus $(\delta^{15}N_{NO3})_0$ values (Figure 2c) shows that all groundwaters fall within the manure/sewage zone, consistent with manure as the dominant NO_3 source across the study area, although some samples have reconstructed $(\delta^{18}O_{NO3})_0$ versus $(\delta^{15}N_{NO3})_0$ values overlapping sewage/manure with NO_3 from synthetic fertilizers and from organic soil. The reconstructed $(\delta^{15}N_{NO3})_0$ values across the investigated field zone range from +2 to +26‰, whereas the reconstructed $(\delta^{18}O_{NO3})_0$ vary between –3 and +9‰ (Table ST4; Figure 2c). The observed ranges of the reconstructed $(\delta^{15}N_{NO3})_0$ and $(\delta^{18}O_{NO3})_0$ values support that a single NO_3 source (i.e., manure here) can exhibit a range of initial $\delta^{15}N_{NO3}$ and $\delta^{18}O_{NO3}$ values, which cannot justify a TEIRD originating from a single point.

5 Discussion

The above results raise concerns regarding some past applications of the concept of TEIRD. Instead, it seems appropriate to proceed with a simplified approach where the correlation between measured $\delta^{18}O_{NO3}$ and $\delta^{15}N_{NO3}$ values in groundwaters is evaluated. If the correlated values plot along a slope $\geq$0.5, the pattern is consistent with an interpretation of denitrification [19,20,41]. However, this is expected to be accurate only for cases where only one NO_3 source exists, with limited variation

between the initial and measured NO_3-isotope values. If a set of samples affected by multiple NO_3 sources are plotted together on the $\delta^{18}O_{NO3}$ versus $\delta^{15}N_{NO3}$ diagram, the expected linear correlation distinguishing denitrification may be not observed, even if denitrification is occurring. An excellent example illustrating this potential confusion when multiple sources of NO_3 exist within a single study area is the study of Paredes et al. [71], although it considers surface waters. A bulk correlation of 29 samples from the Doñana wetland (Spain) does not show a significant linear trendline between $\delta^{18}O_{NO3}$ and $\delta^{15}N_{NO3}$ values to justify the occurrence of denitrification (Figure SF1k), whereas this appears when the samples are constrained by their contamination sources [71]. For instance, samples PDpal, PDmim and STca (identified with green circles in Figure SF1k) show a trendline having a slope of 1; these samples were collected exclusively at sampling sites where chemical fertilizers represent the main potential NO_3 source. Beyond these considerations, it seems that the concept of TEIRD can still be used, but only after evaluating the following three aspects:

(i) The potential NO_3 sources in the groundwater system should be identified not only with NO_3 isotope-based methods (e.g., the $\delta^{18}O_{NO3}$ versus $\delta^{15}N_{NO3}$ plot, Figure 1), but also with tracking the history of the land use combined with groundwater age dating because the dominant NO_3 source can shift over time [52,72]. Identifying the NO_3 sources with their history allows investigators to more accurately determine the initial endmembers of the current NO_3 groundwater contamination at the investigated site.

(ii) The initial isotopic compositions of the identified NO_3 sources should be measured or reconstructed. The mathematical and numerical models described above for reconstructing the $(\delta^{15}N_{NO3})_0$ and $(\delta^{18}O_{NO3})_0$ values with data from case studies reveal that a given single NO_3 source is commonly characterized by a range for $\delta^{15}N_{NO3}$ and $\delta^{18}O_{NO3}$ values, consistent with observations from field data (e.g. Lorette et al. [55]). Accordingly, the endmember data of a given NO_3 source typically plot within a square to rectangular zone on a plot of $\delta^{18}O_{NO3}$ versus $\delta^{15}N_{NO3}$, and not as a single point as some earlier studies suggest (see example in Figure SF1i).

(iii) The slope of the denitrification trend should be assessed from the regressive correlation of the measured $\delta^{18}O_{NO3}$ and $\delta^{15}N_{NO3}$ values of groundwater samples. Subsequently, two trendlines delineating the TEIRD can be traced from the square/rectangular zone of the reconstructed $(\delta^{15}N_{NO3})_0$ and $(\delta^{18}O_{NO3})_0$ values, but using slopes computed from data of the investigated site, rather than theoretical slopes such as 0.5 from Böttcher et al. [20]. It is important to mention here that each NO_3 source can have its own specific TEIRD, although denitrification trendlines for multiple NO_3 sources in the same study area can have the same slope. Indeed, groundwater samples from the CA site, that are indicated with black circles in Figure SF1j, have different NO_3-isotope compositions corresponding to different NO_3 sources, but could be aligned along a same sloped trendline linking the NO_3-isotope compositions. However, this cannot be generalized. Indeed, Otero et al. [65] observed that, within the Osona aquifer, some groundwater samples exhibited a slope differing from that observed for other samples. Alternatively, the slope of the denitrification trend can be assessed from the correlation of the measured $\delta^{18}O_{NO3}$ and $\delta^{15}N_{NO3}$ values belonging to the same NO_3 source.

Among the three above considerations, the most critical point is the reconstruction of the $(\delta^{15}N_{NO3})_0$ and $(\delta^{18}O_{NO3})_0$ values. As the Heaton et al. [60] and the Böhlke et al. [67] models integrate approaches for reconstructing only $(\delta^{15}N_{NO3})_0$, their application to define TEIRD is limited unless these models are combined with the approach for reconstructing the theoretical $(\delta^{18}O_{NO3})_0$. Furthermore, both the Heaton et al. [60] and the Böhlke et al. [67] models require that the amount of N_2 derived from denitrification be determined, which involves knowledge of how much of the N_2 is naturally occurring (i.e., enters during recharge), thus requiring the analytical measurement of inert gas concentrations such as Ar or He. Mariotti et al. [73] concluded that the use of $\delta^{15}N_{N2}$ to investigate denitrification processes is challenging because of the difficulty of collection and preservation of N_2 gas without atmospheric contamination, and the complications associated with accurate determination of the fraction of N_2 produced by denitrification [66], among other impediments. While several studies have measured dissolved gases for other research interests (e.g., groundwater residence time determination), most have not measured N_2 and are not directed towards NO_3

groundwater studies. For these reasons, the Heaton et al. [60] and the Böhlke et al. [67] models have limited applications, although both models have successfully been implemented in some investigations [52,74]. Integrating sophisticated experimental methods for measuring the fraction of N_2 produced by denitrification and developing N_2 based-mathematical models that allow the reconstruction of $(\delta^{18}O_{NO3})_0$ is a prospective research topic of interest that could contribute to a more effective use of the TEIRD concept.

To reconstruct theoretical $(\delta^{18}O_{NO3})_0$ values (section 4.3), many case studies revealed that the $\delta^{18}O_{NO3\ (theoretical)}$ values, evaluated for groundwater subjected to denitrification, are consistent as reconstructed values tend to be lower than those measured in groundwater, supporting enrichment of $^{18}O_{NO3}$ due to denitrification [15,43,75]. However, other case studies where $\delta^{18}O_{NO3\ (theoretical)}$ values are lower than those measured have been attributed to other mechanisms such as evaporation, respiration, and increased precipitation [76–79], whereas $\delta^{18}O_{NO3\ (theoretical)}$ values greater than those measured have been assigned to kinetic O isotope fractionation during nitrification and also hypothesized to derive from isotopic exchange of O atoms between the NO_2 intermediate and H_2O [80–82]. It is important to note that the application of the theoretical $(\delta^{18}O_{NO3})_0$ model (Equation 6) is constrained with critical assumptions including (i) the proportion of dissolved oxygen from water and that from O_2 are constant, (ii) the incorporation of oxygen atoms from water or O_2 occurs without O isotope fractionation, (iii) microbes and bulk soil water use identical $\delta^{18}O_{H2O}$, and (vi) microbes use $\delta^{18}O_{O2}$ that is identical to that of atmospheric O_2 [66]. Therefore, the assessed $\delta^{18}O_{NO3\ (theoretical)}$ values constitute an approximate evaluation because some investigations indicated that other processes may influence the isotopic composition of dissolved NO_3 [26,82].

Sampling identified primary NO_3 sources in a targeted study area and measuring their $\delta^{15}N_{NO3}$ and $\delta^{18}O_{NO3}$ values can be an effective approach for determining the $(\delta^{15}N_{NO3})_0$ and $(\delta^{18}O_{NO3})_0$ values. However, a given isotopic signature of the NO_3 source can be already affected by local biogeochemical processes altering its original isotopic signature. For example, NH_4 volatilization after manure spreading is known to increase the $\delta^{15}N_{NO3}$ values. Thus, NH_4

volatilization potentially contributes to the extent isotopic range of $\delta^{15}N_{NO3}$ and $\delta^{18}O_{NO3}$ observed in groundwater affected by manure. In arid and semiarid environments, NH_4 volatilization may affect synthetic fertilizers, so that NO_3 originated from this source does not display a typical $\delta^{15}N_{NO3}$ isotopic signature [83]. The other available mathematical and numerical approaches for reconstructing $(\delta^{15}N_{NO3})_0$ and $(\delta^{18}O_{NO3})_0$ values are based on sampled groundwaters with isotopic composition that could be biased due to potential mixing of different NO_3 sources and kinetic isotopic fractionation process [12,84]. The occurrence of these processes can consequently affect the reconstructed $(\delta^{15}N_{NO3})_0$ and $(\delta^{18}O_{NO3})_0$ values, leading to uncertainty of the reconstructed isotopic compositions. Indeed, the $(\delta^{15}N_{NO3})_0$ and $(\delta^{18}O_{NO3})_0$ values reconstructed with the Rayleigh-based model from a set of data (i.e., spring samples from a rural area collected during low water condition [55]) do not all fall inside the dashed square zone representing the measured NO_3 source (i.e., cultivated soil) endmembers (Figure 2d). This shows the challenge of using other approaches for reconstructing $(\delta^{15}N_{NO3})_0$ and $(\delta^{18}O_{NO3})_0$ values rather than measuring the primary identified NO_3 sources. Future targeted research focusing on how integrating potential mixing of different NO_3 sources and kinetic isotopic fractionation process in models for reconstructing $(\delta^{15}N_{NO3})_0$ and $(\delta^{18}O_{NO3})_0$ values can contribute to a more effective use of the TEIRD concept.

The plot of measured $\delta^{18}O_{NO3}$ versus $\delta^{15}N_{NO3}$ values of groundwater, from three field zones of the same study area investigated by Otero et al. [65], provides evidence for denitrification given the observed positive correlation between the plotted data (Figure 3a). Otero et al. [65] indicated that most groundwater samples with higher NO_3 concentrations in the three field zones plot within the same square shown on Figure 3b-d with lower $\delta^{15}N_{NO3}$ and $\delta^{18}O_{NO3}$ values. The authors considered that the samples falling in the square lacked clear evidence of denitrification and rather represent an endmember with a single isotopic composition (i.e., $\delta^{15}N_{NO3}$ = +15‰ and $\delta^{18}O_{NO3}$ = +5‰) corresponding to the values of the most $^{15}N_{NO3}$ and $^{18}O_{NO3}$ enriched endmember of the determined square (Figure 3b-d). This single isotopic composition was assumed to be representative of the source of NO_3 because there is one predominant NO_3 source across the study area, namely manure.

Assuming a single isotopic composition for the NO_3 source can lead to underestimation of the TEIRD extent because a single isotopic composition should be reflected by a single denitrification trendline instead of a range constrained by two denitrification trendlines originating from the extremes of the determined square. Furthermore, by using the Rayleigh model-based approach for reconstructing $(\delta^{15}N_{NO3})_0$ and $(\delta^{18}O_{NO3})_0$ values, it is observed for the zone 3 data that there is a shift between the measured $\delta^{15}N_{NO3}$ and $\delta^{18}O_{NO3}$ values and the reconstructed $(\delta^{15}N_{NO3})_0$ and $(\delta^{18}O_{NO3})_0$ values (see the shift between the triangles and circles in Figure 2c). This shift consequently relocates the square corresponding to non-denitrified samples in Figure 3d. However, the reconstructed values here include all samples, without distinguishing those that undergo denitrification from those that are not initially affected by denitrification. Alternatively, before reconstructing the $(\delta^{15}N_{NO3})_0$ and $(\delta^{18}O_{NO3})_0$ values for a given groundwater system, it would be necessary to distinguish samples without evidence of denitrification and to discard them from the evaluation of TEIRD. This can be undertaken based on DO data as denitrification is expected to occur in anaerobic conditions having limited DO availability (concentrations <4 mg/L) [85]. Nonetheless, DO data would only be useful where long-term DO data are available, for a given studied aquifer, because groundwater DO can change seasonally [85] and achieve high values that are not suitable for effective denitrification. Also, denitrification is reported in moderately oxic/anoxic subsurface zones along the flow-paths featuring reducing conditions [70,83], with potential mixing of various NO_3 sources generating $\delta^{15}N_{NO3}$ and $\delta^{18}O_{NO3}$ values also behaving with a slope similar to denitrification [19,23], which make defining TEIRD challenging. Research focusing on how to effectively distinguish water samples that have clearly not been affected by denitrification is needed to advance the application of the TEIRD concept.

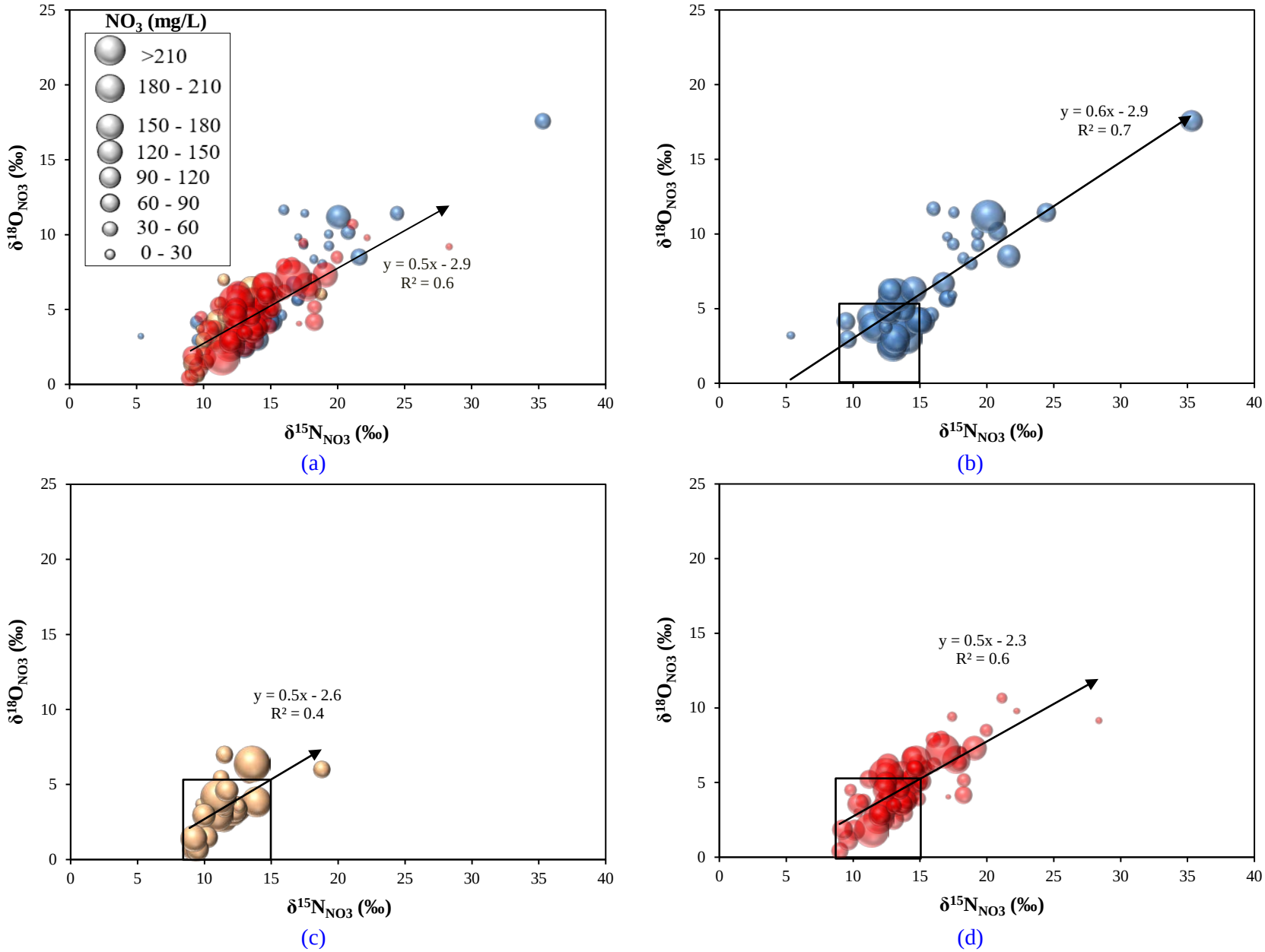

Figure 3. Plot of $\delta^{18}O_{NO3}$ versus $\delta^{15}N_{NO3}$ values for samples belonging to (a) a study area including three different field zones; (b) samples belonging to field zone 1; (c) samples belonging to field zone 2; and (d) samples belonging to field zone 3 (data from Otero et al. [65]). In (b), (c) and (d), the squares were assumed to correspond to the isotopic composition of NO_3 source (i.e., manure). Groundwater samples are shown with different bubble size as indicative of different NO_3 concentrations.

6 Conclusion

In this paper, a demonstration of the commonly observed shortcomings with the application of the TEIRD concept is provided. First, many studies distinguished partially denitrified groundwaters by using a TEIRD concept that combines two sloped straight lines originated from a single point, corresponding to $(\delta^{15}N_{NO3})_0$ and $(\delta^{18}O_{NO3})_0$ values, whereas this concept was actually introduced to show two potential denitrification trends (i.e., slopes) that are not together valid for the same aquifer system. Second, many studies applied the TEIRD concept relying on a single NO_3 source, even though multiple NO_3 sources exist. Third, less attention was paid to the initial $(\delta^{15}N_{NO3})_0$ and $(\delta^{18}O_{NO3})_0$ values with most studies introducing an assumed initial NO_3-isotope composition without justification, i.e., without measuring the $\delta^{15}N_{NO3}$ and $\delta^{18}O_{NO3}$ values of the NO_3 source or reconstructing mathematically/numerically the initial $(\delta^{15}N_{NO3})_0$ and $(\delta^{18}O_{NO3})_0$ values of the NO_3 source. All of these assumptions can lead not only to an uncertain delineation of the TEIRD, but also to an uncertain classification of denitrified groundwater. Alternatively, future studies focusing on denitrification within groundwater systems can confirm the occurrence of denitrification when the correlation of $\delta^{18}O_{NO3}$ with $\delta^{15}N_{NO3}$ values plot along slope ≥ 0.5 with one potential NO_3 source. Nonetheless, it is still useful to apply the TEIRD concept when comprehensive information on the three following aspects are available: (i) information on all potential previous/current sources of NO_3 present in the investigated groundwater system by combining relevant isotopic tracers**,** groundwater age dating, and the history of the land use; (ii) information on the measured or reconstructed initial NO_3-isotope compositions of the identified NO_3 sources; and (iii) information on the slope of the denitrification trend according to the measured $\delta^{15}N_{NO3}$ and $\delta^{18}O_{NO3}$ values in groundwater. The measured or reconstructed initial NO_3 isotopic compositions of each NO_3 source can be constrained under a square/rectangular domain, from which two denitrification trendlines having the assessed denitrification slope can be traced for delineating the TEIRD. Each NO_3 source could have a specific square/rectangular domain of its endmembers; consequently, each NO_3 source

could have a specific TEIRD, although the denitrification trendlines for multiple NO_3 sources in the same pool can be of the same slope, but this can not be generalized for all groundwater systems.

Supporting Information

Supporting information include a set of Figures related to denitrification trends and Tables with variable measured and simulated data.

Acknowledgements

The authors acknowledge the financial support from the *Spain Ministry of Science and Innovation* (Grant number PID2022-139911OB-C4-01 held by Prof. Neus Otero). The authors would like to thank Dr. Carol Kendall (former research scientist at the United States Geological Survey), Dr. Leonard Wassenaar (research scientist at the WasserCluster Lunz Biological Research Station, Austria), and Dr. Tim Heaton (former researcher at the British Geological Survey) for their advice and suggestions helping to improve this manuscript before its submission. The authors thank Dr. Sarah Bourke from the University of Western Australia for her help in providing the data of the agricultural areas in Alberta (Canada).

References

(1) Matiatos, I.; Wassenaar, L. I.; Monteiro, L. R.; Venkiteswaran, J. J.; Gooddy, D. C.; Boeckx, P.; Sacchi, E.; Yue, F.; Michalski, G.; Alonso-Hernandez, C.; Biasi, C.; Bouchaou, L.; Edirisinghe, N. V.; Fadhullah, W.; Fianko, J. R.; García-Moya, A.; Kazakis, N.; Li, S. L.; Luu, M. T. N.; Priyadarshanee, S.; Re, V.; Rivera, D. S.; Romanelli, A.; Sanyal, P.; Tamooh, F.; Trinh, D. A.; Walters, W.; Welti, N. Global Patterns of Nitrate Isotope Composition in Rivers and Adjacent Aquifers Reveal Reactive Nitrogen Cascading. *Commun. Earth Environ.* **2021**, *2* (52), 1–10.

(2) Galloway, J. N.; Dentener, F. J.; Capone, D. G.; Boyer, E. W.; Howarth, R. W.; Seitzinger, S. P.; Asner, G. P.; Cleveland, C. C.; Green, P. A.; Holland, E. A.; Karl, D. M.; Michaels, A. F.; Porter, J. H.; Townsend, A. R.; Vöosmarty, C. J. Nitrogen Cycles: Past, Present, and Future. *Biogeochemistry* **2004**, *70*, 153–226.

(3) Rabalais, N. N. Nitrogen in Aquatic Ecosystems. *AMBIO A J. Hum. Environ.* **2002**, *31* (2), 102–112.

(4) Torres-Martínez, J. A.; Mora, A.; Knappett, P. S. K.; Ornelas-Soto, N.; Mahlknecht, J. Tracking Nitrate and Sulfate Sources in Groundwater of an Urbanized Valley Using a Multi-Tracer Approach Combined with a Bayesian Isotope Mixing Model. *Water Res.* **2020**, *182* (115962), 1–16.

(5) Puig, R.; Soler, A.; Widory, D.; Mas-Pla, J.; Domènech, C.; Otero, N. Characterizing Sources and Natural Attenuation of Nitrate Contamination in the BaixTer Aquifer System (NE Spain) Using a Multi-Isotope Approach. *Sci. Total Environ.* **2017**, *580*, 518–532.

(6) Boumaiza, L.; Chesnaux, R.; Drias, T.; Walter, J.; Huneau, F.; Garel, E.; Knoeller, K.; Stumpp, C. Identifying Groundwater Degradation Sources in a Mediterranean Coastal Area

Experiencing Significant Multi-Origin Stresses. *Sci. Total Environ.* **2020**, *746* (141203), 1–20.

(7) Boumaiza, L.; Walter, J.; Chesnaux, R.; Huneau, F.; Garel, E.; Erostate, M.; Johannesson, K. H.; Vystavna, Y.; Bougherira, N.; Bordeleau, G.; Stotler, R. L.; Blarasin, M.; Gutierrez, M.; Knöller, K.; Stumpp, C. Multi-Tracer Approach to Understand Nitrate Contamination and Groundwater-Surface Water Interactions in the Mediterranean Coastal Area of Guerbes-Senhadja, Algeria. *J. Contam. Hydrol.* **2022**, *251* (104098), 1–16.

(8) Blarasin, M.; Matiatos, I.; Cabrera, A.; Lutri, V.; Giacobone, D.; Quinodoz, F. B.; Matteoda, E.; Eric, C.; Felizzia, J.; Albo, J. G. Characterization of Groundwater Dynamics and Contamination in an Unconfined Aquifer Using Isotope Techniques to Evaluate Domestic Supply in an Urban Area. *J. South Am. Earth Sci.* **2021**, *110* (103360), 1–13.

(9) Briand, C.; Sebilo, M.; Louvat, P.; Chesnot, T.; Vaury, V.; Schneider, M.; Plagnes, V. Legacy of Contaminant N Sources to the NO3- Signature in Rivers: A Combined Isotopic (Delta N-15-NO3-, Delta O-18-NO3-, Delta B-11) and Microbiological Investigation. *Sci. Rep.* **2017**, *7* (41703), 1–11.

(10) Gooddy, D. C.; Lapworth, D. J.; Bennett, S. A.; Heaton, T. H. E.; Williams, P. J.; Surridge, B. W. J. A Multi-Stable Isotope Framework to Understand Eutrophication in Aquatic Ecosystems. *Water Res.* **2016**, *88*, 623–633.

(11) Matiatos, I.; Lazogiannis, K.; Papadopoulos, A.; Skoulikidis, N. T.; Boeckx, P.; Dimitriou, E. Stable Isotopes Reveal Organic Nitrogen Pollution and Cycling from Point and Non-Point Sources in a Heavily Cultivated (Agricultural) Mediterranean River Basin. *Sci. Total Environ.* **2023**, *901* (166455), 1–13.

(12) Soto, D. X.; Koehler, G.; Wassenaar, L. I.; Hobson, K. A. Spatio-Temporal Variation of Nitrate Sources to Lake Winnipeg Using N and O Isotope (Δ15N, Δ18O) Analyses. *Sci. Total Environ.* **2019**, *647*, 486–493.

(13) Boumaiza, L.; Walter, J.; Chesnaux, R.; Zahi, F.; Huneau, F.; Garel, E.; Stotler, R. L.; Bordeleau, G.; Drias, T.; Johannesson, K. H.; Vystavna, Y.; Re, V.; Knöller, K.; Stumpp, C. Combined Effects of Seawater Intrusion and Nitrate Contamination on Groundwater in Coastal Agricultural Areas: A Case from the Plain of the El-Nil River (North-Eastern Algeria). *Sci. Total Environ.* **2022**, *851* (158153), 1–13.

(14) Matiatos, I.; Moeck, C.; Vystavna, Y.; Marttila, H.; Orlowski, N.; Jessen, S.; Evaristo, J.; Sebilo, M.; Koren, G.; Dimitriou, E.; Müller, S.; Panagopoulos, Y.; Stockinger, M. P. Nitrate Isotopes in Catchment Hydrology: Insights, Ideas and Implications for Models. *J. Hydrol.* **2023**, *626* (130326), 1–17.

(15) Boumaiza, L.; Ben-Ammar, S.; Chesnaux, R.; Stotler, R. L.; Mayer, B.; Huneau, F.; Johannesson, K. H.; Levison, J.; Knöller, K.; Stumpp, C. Nitrate Sources and Transformation Processes in Groundwater of a Coastal Area Experiencing Various Environmental Stressors. *J. Environ. Manage.* **2023**, *345* (118803), 1–11.

(16) Mayer, B.; Matiatos, I. Nutrient Dynamics in Rivers and Lakes. In *In Editor(s): Ariel Anbar, Dominique Weis, Treatise on Geochemistry (Third edition), Elsevier, ISBN 9780323997638.*; 2024; pp 155–178.

(17) Asamoto, C. K.; Rempfert, K. R.; Lu, V. H.; Younkin, A. D.; Kopf, S. H. Enzyme-Specific Coupling of Oxygen and Nitrogen Isotope Fractionation of the Nap and Nar Nitrate Reductases. *Environ. Sci. Technol.* **2021**, *55*, 5537–5546.

(18) Granger, J.; Wankel, S. D. Isotopic Overprinting of Nitrification on Denitrification as a Ubiquitous and Unifying Feature of Environmental Nitrogen Cycling. *Proc. Natl. Acad. Sci. U. S. A.* **2016**, *113* (42), 6391–6400.

(19) Kendall, C.; Elliott, E. M.; Wankel, S. D. Tracing Anthropogenic Inputs of Nitrogen to Ecosystems. *Stable Isot. Ecol. Environ. Sci. Second Ed. Blackwell Publ.* **2008**, 375–449.

(20) Böttcher, J.; Strebel, O.; Voerkelius, S.; Schmidt, H. L. Using Isotope Fractionation of Nitrate-Nitrogen and Nitrate-Oxygen for Evaluation of Microbial Denitrification in a Sandy

Aquifer. *J. Hydrol.* **1990**, *114* (3–4), 413–424.
(21) Aravena, R.; Robertson, W. D. Use of Multiple Isotope Tracers to Evaluate Denitrification in Ground Water: Study of Nitrate from a Large-Flux Septic System Plume. *Ground Water* **1998**, *36* (6), 975–982.
(22) Amberger, A.; Schmidt, H. L. The Natural Isotope Abundance of Nitrate as an Indicator for Its Origin. *Geochim. Cosmochim. Acta* **1987**, *51*, 2699–2705.
(23) Mayer, B.; Boyer, E. W.; Goodale, C.; Jaworski, N. A.; Van Breemen, N.; Howarth, R. W.; Seitzinger, S.; Billen, G.; Lajtha, K.; Nadelhoffer, K.; Van Dam, D.; Hetling, L. J.; Nosal, M.; Paustian, K. Sources of Nitrate in Rivers Draining Sixteen Watersheds in the Northeastern U.S.: Isotopic Constraints. *Biogeochemistry* **2002**, *57* (58), 171–197.
(24) Granger, J.; Sigman, D. M.; Needoba, J. A.; Harrison, P. J. Coupled Nitrogen and Oxygen Isotope Fractionation of Nitrate during Assimilation by Cultures of Marine Phytoplankton. *Limnol. Oceanogr.* **2004**, *49* (5), 1763–1773.
(25) Buchwald, C.; Casciotti, K. L. Oxygen Isotopic Fractionation and Exchange during Bacterial Nitrite Oxidation. *Limnol. Oceanogr.* **2010**, *55* (3), 1064–1074.
(26) Casciotti, K. L.; McIlvin, M.; Buchwald, C. Oxygen Isotopic Exchange and Fractionation during Bacterial Ammonia Oxidation. *Limnol. Oceanogr.* **2010**, *55* (2), 753–762.
(27) Mobius, J. Isotope Fractionation during Nitrogen Remineralization (Ammonification): Implications for Nitrogen Isotope Biogeochemistry. *Geochim. Cosmochim. Acta* **2013**, *105*, 422–432.
(28) Sigman, D. M.; Casciotti, K. L.; Andreani, M.; Barford, C.; Galanter, M.; Böhlke, J. K. A Bacterial Method for the Nitrogen Isotopic Analysis of Nitrate in Seawater and Freshwater. *Anal. Chem.* **2001**, *73*, 4145–4153.
(29) Casciotti, K. L.; Sigman, D. M.; Hastings, M. G.; Böhlke, J. K.; Hilkert, A. Measurement of the Oxygen Isotopic Composition of Nitrate in Seawater and Freshwater Using the Denitrifier Method. *Anal. Chem.* **2002**, *74*, 4905–4912.
(30) Mengis, M.; Schiff, S. L.; Harris, M.; English, M. C.; Aravena, R.; Elgood, R. J.; MacLean, A. Multiple Geochemical and Isotopic Approaches for Assessing Ground Water NO3 - Elimination in a Riparian Zone. *Ground Water* **1999**, *37* (3), 448–457.
(31) Wenk, C. B.; Zopfi, J.; Blees, J.; Veronesi, M.; Niemann, H.; Lehmann, M. F. Community N and O Isotope Fractionation by Sulfide-Dependent Denitrification and Anammox in a Stratified Lacustrine Water Column. *Geochim. Cosmochim. Acta* **2014**, *125*, 551-563.
(32) Cey, E. E.; Rudolph, D. L.; Aravena, R.; Parkin, G. Role of the Riparian Zone in Controlling the Distribution and Fate of Agricultural Nitrogen near a Small Stream in Southern Ontario. *J. Contam. Hydrol.* **1999**, *37*, 45–67.
(33) Swart, P. K.; Evans, S.; Capo, T.; Altabet, M. A. The Fractionation of Nitrogen and Oxygen Isotopes in Macroalgae during the Assimilation of Nitrate. *Biogeosciences* **2014**, *11* (21), 6147–6157.
(34) Casciotti, K. L.; Buchwald, C.; McIlvin, M. Implications of Nitrate and Nitrite Isotopic Measurements for the Mechanisms of Nitrogen Cycling in the Peru Oxygen Deficient Zone. *Deep Sea Res. Part II Top. Stud. Oceanogr.* **2013**, *80*, 78–93.
(35) Gaye, B.; Nagel, B.; Dähnke, K.; Rixen, T.; Emeis, K. C. Evidence of Parallel Denitrification and Nitrite Oxidation in the ODZ of the Arabian Sea from Paired Stable Isotopes of Nitrate and Nitrite. *Global Biogeochem. Cycles* **2013**, *27*, 1059–1071.
(36) Rafter, P. A.; DiFiore, P. J.; Sigman, D. M. Coupled Nitrate Nitrogen and Oxygen Isotopes and Organic Matter Remineralization in the Southern and Pacific Oceans: Nitrate Isotopes and Remineralization. *J. Geophys. Res. Ocean.* **2013**, *118*, 4781–4794.
(37) Matiatos, I.; Monteiro, L. R.; Sebilo, M.; Soto, D. X.; Gooddy, D. C.; L.I., W. Isotopes Reveal the Moderating Role of Ammonium on Global Riverine Water Nitrogen Cycling. *ACS EST Water* **2024**, *4* (4), 1451–1459.
(38) Xuan, Y. X.; Tang, C. Y.; Cao, Y. J. Mechanisms of Nitrate Accumulation in Highly

Urbanized Rivers: Evidence from Multi-Isotopes in the Pearl River Delta, China. *J. Hydrol.* **2020**, *587* (124924), 1–11.
(39) Weitzman, J. N.; Brooks, J. R.; Mayer, M. P.; Rugh, W. D.; Compton, J. E. Coupling the Dual Isotopes of Water (Δ2H and Δ18O) Nitrate (Δ15N and Δ18O): A New Framework for Classifying Current and Legacy Groundwater Pollution. *Environ. Res. Lett.* **2021**, *16* (045008), 1–13.
(40) Höener, P.; Imfeld, G. Quantification of Lambda (Λ) in Multi-Elemental Compound-Specific Isotope Analysis. *Chemosphere* **2021**, *267* (129232), 1–5.
(41) Fukada, T.; Hiscock, K. M.; Dennis, P. F.; Grischek, T. A Dual Isotope Approach to Identify Denitrification in Groundwater at a River-Bank Infiltration Site. *Water Res.* **2003**, *37* (13), 3070–3078.
(42) Devito, K. J.; Fitzgerald, D.; Hill, A. R.; Aravena, R. Nitrate Dynamics in Relation to Lithology and Hydrologic Flow Path in a River Riparian Zone. *J. Environ. Qual.* **2000**, *29*, 1075–1084.
(43) Blarasin, M.; Cabrera, A.; Ioannis Matiatos, I.; Becher Quinodóz, F.; Giuliano Albo, J.; Lutri, V.; Matteoda, E.; Panarello, H. Comparative Evaluation of Urban versus Agricultural Nitrate Sources and Sinks in an Unconfined Aquifer by Isotopic and Multivariate Analyses. *Sci. Total Environ.* **2020**, *741* (140374), 1–15.
(44) Jin, Z.; Pan, Z.; Jin, M.; Li, F.; Wan, Y.; Gu, B. Determination of Nitrate Contamination Sources Using Isotopic and Chemical Indicators in an Agricultural Region in China. *Agric. Ecosyst. Environ.* **2012**, *155*, 78–86.
(45) Kim, K. H.; Yun, S. T.; Mayer, B.; Lee, J. H.; Kim, T. S.; Kim, H. K. Quantification of Nitrate Sources in Groundwater Using Hydrochemical and Dual Isotopic Data Combined with a Bayesian Mixing Model. *Agric. Ecosyst. Environ.* **2015**, *199*, 369–381.
(46) Pastén-Zapata, E.; Ledesma-Ruiz, R.; Harter, T.; Ramírez, A. I.; Mahlknecht, J. Assessment of Sources and Fate of Nitrate in Shallow Groundwater of an Agricultural Area by Using a Multi-Tracer Approach. *Sci. Total Environ.* **2014**, No. 470–471, 855–864.
(47) Torres-Martínez, J. A.; Mora, A.; Mahlknecht, J.; Daessle, L. W.; Cervantes-Aviles, P. A.; Ledesma-Ruiz, R. Estimation of Nitrate Pollution Sources and Transformations in Groundwater of an Intensive Livestock-Agricultural Area (Comarca Lagunera), Combining Major Ions, Stable Isotopes and MixSIAR Model. *Environ. Pollut.* **2021**, *269* (115445), 1–12.
(48) Niu, X.; Jia, X.; Yang, X.; Wang, J.; Wei, X.; Wu, L.; Shao, M. Tracing the Sources and Fate of NO3− in the Vadose Zone− Groundwater System of a Thousand-Year-Cultivated Region. *Environ. Sci. Technol.* **2022**, *56*, 9335–9345.
(49) Zaryab, A.; Nassery, H. R.; Knoeller, K.; Alijani, F.; Minet, E. Determining Nitrate Pollution Sources in the Kabul Plain Aquifer (Afghanistan) Using Stable Isotopes and Bayesian Stable Isotope Mixing Model. *Sci. Total Environ.* **2022**, *823* (153749), 1–13.
(50) Ding, K.; Zhang, Y.; Zhang, H.; Yu, C.; Li, X.; Zhang, M.; Zhang, Z.; Yang, Y. Tracing Nitrate Origins and Transformation Processes in Groundwater of the Hohhot Basin's Piedmont Strong Runoff Zone through Dual Isotopes and Hydro-Chemical Analysis. *Sci. Total Environ.* **2024**, *919* (170799), 1–17.
(51) Zaryab, A.; Alijani, F.; Knoeller, K.; Minet, E.; Musavi, S. F.; Ostadhashemi, Z. Identification of Groundwater Nitrate Sources in an Urban Aquifer (Alborz Province, Iran) Using a Multi-parameter Approach. *Environ. Geochem. Health* **2024**, *46* (100), 1–17.
(52) Green, C. T.; Puckett, L. J.; Böhlke, J. K.; Bekins, B. A.; Phillips, S. P.; Kauffman, L. J.; Denver, J. M.; Johnson, H. M. Limited Occurrence of Denitrifi Cation in Four Shallow Aquifers in Agricultural Areas of the United States. *J. Environ. Qual.* **2008**, *37* (3), 994–1009.
(53) Martinelli, G.; Dadomo, A.; De Luca, D. A.; Mazzola, M.; Lasagna, M.; Pennisi, M.; Pilla, G.; Sacchi, E.; Saccon, P. Nitrate Sources, Accumulation and Reduction in Groundwater

from Northern Italy: Insights Provided by a Nitrate and Boron Isotopic Database. *Appl. Geochemistry* **2018**, *91*, 23–35.
(54) Wang, M.; Lu, B.; Wang, J.; Zhang, H.; Guo, L.; Lin, H. Using Dual Isotopes and a Bayesian Isotope Mixing Model to Evaluate Nitrate Sources of Surface Water in a Drinking Water Source Watershed, East China. *Water* **2016**, *8* (355), 1–16.
(55) Lorette, G.; Sebilo, M.; Buquet, D.; Lastennet, R.; Denis, A.; Peyraube, N.; Charriere, V.; Studer, J. C. Tracing Sources and Fate of Nitrate in Multilayered Karstic Hydrogeological Catchments Using Natural Stable Isotopic Composition (Δ15N-NO3 and Δ18O-NO3). Application to the Toulon Karst System (Dordogne, France). *J. Hydrol.* **2022**, *610* (127972), 1–14.
(56) Ye, H.; Han, Z.; Wu, P.; Zha, X.; Li, X.; Hou, E.; Cao, Y.; Tang, C.; Zhang, R.; Sardans, J.; Penuelas, J. Disentangling Sources and Transformation Mechanisms of Nitrogen, Sulfate, and Carbon in Water of a Karst Critical Zone. *Sci. Total Environ.* **2024**, *922* (171310), 1–13.
(57) Bao, Y.; Sun, M.; Wang, Y.; Hu, M.; Hu, P.; Wu, L.; Huang, W.; Li, S.; Wen, J.; Wang, Z. J.; Zhang, Q.; Wu, N. Nitrate Transformation and Source Tracking of Yarlung Tsangpo River Using a Multi-Tracer Approach Combined with Bayesian Stable Isotope Mixing Model. *Environ. Res.* **2024**, *252* (118925), 1–9.
(58) Duan, L.; Wu, Y.; Fan, J.; Ye, F.; Xie, C.; Fu, X.; Sun, Y. Identification of Nitrogen Pollution Sources and Transport Transformation Processes in Groundwater of Different Landforms Using C, H, N, and O Isotope Techniques: An Example from the Lower Weihe River. *Environ. Sci. Pollut. Res.* **2023**, *30*, 29442–29457.
(59) Kasem, A. M.; Xu, Z.; Jiang, H.; Liu, W.; Zhang, J.; Nosair, A. M. Nitrate Source and Transformation in Groundwater under Urban and Agricultural Arid Environment in the Southeastern Nile Delta, Egypt. *Water* **2024**, *6* (22), 1–22.
(60) Heaton, T. H. E.; Talma, A. S.; Vogle, J. C. Origin and History of Nitrate in Confined Groundwater in the Western Kalahari. *J. Hydrol.* **1983**, *62*, 243–262.
(61) Mariotti, A.; Germon, J. C.; Hubert, P.; Kaiser, P.; Letolle, R.; Tardieux, A.; Tardieux, P. Experimental Determination of Nitrogen Kinetic Isotope Fractionation: Some Principles; Illustration for the Denitrification and Nitrification Processes. *Plant Soil* **1981**, *62*, 413–430.
(62) Edmunds, W. M.; Shand, P. *Natural Groundwater Quality*; Blackwell Publishing Ltd, Malden. Ferguson, G.C., 2008.
(63) Appelo, C. A. J.; Postma, D. *Geochemistry, Groundwater and Pollution, Second Edition*; 2nd Edition, Balkema, Leiden, The Netherlands., 2005.
(64) Bourke, S. A.; Iwanyshyn, M.; Kohn, J.; Hendry, M. J. Sources and Fate of Nitrate in Groundwater at Agricultural Operations Overlying Glacial Sediments. *Hydrol. Earth Syst. Sci.* **2019**, *23*, 1355–1373.
(65) Otero, N.; Torrento, C.; Soler, A.; Mencio, A.; Mas-Pla, J. Monitoring Groundwater Nitrate Attenuation in a Regional System Coupling Hydrogeology with Multi-Isotopic Methods: The Case of Plana de Vic (Osona, Spain). *Agric. Ecosyst. Environ.* **2009**, *133*, 103–113.
(66) Kendall, C. Tracing Nitrogen Sources and Cycling in Catchments. *Isot. Tracers Catchment Hydrol.* **1998**, 519–576.
(67) Böhlke, J. K.; Wanty, R.; Tuttle, M.; Delin, G.; Landon, M. Denitrification in the Recharge Area and Discharge Area of a Transient Agricultural Nitrate Plume in a Glacial Outwash Sand Aquifer, Minnesota. *Water Resour. Res.* **2002**, *38* (7), 1–25.
(68) Heaton, T. H. E. Isotopic Studies of Nitrogen Pollution in the Hydrosphere and Atmosphere–A Review. *Chem. Geol.* **1986**, *59*, 87–102.
(69) Fogg, G. .; Rolston, D. E.; Decker, D. L.; Louie, D. T.; Grismer, M. E. Spatial Variation in Nitrogen Isotope Values beneath Nitrate Contamination Sources. *Ground Water* **1998**, *36*, 418–426.
(70) Kroopnick, P. M.; Craig., H. Atmospheric Oxygen: Isotopic Composition and Solubility

Fractionation. *Science (80-.).* **1972**, *175*, 54–55.
(71) Paredes, I.; Otero, N.; Soler, A.; Green, A. J.; Soto, D. X. Agricultural and Urban Delivered Nitrate Pollution Input to Mediterranean Temporary Freshwaters. *Agric. Ecosyst. Environ.* **2020**, *294* (106859), 1–12.
(72) Re, V.; Sacchi, E.; Kammoun, S.; Tringali, C.; Trabelsi, R.; Zouari, K.; Daniele, S. Integrated Socio-Hydrogeological Approach to Tackle Nitrate Contamination in Groundwater Resources. The Case of Grombalia Basin (Tunisia). *Sci. Total Environ.* **2017**, *593*, 664–676.
(73) Mariotti, A.; Landreau, A.; Simon, B. 15N Isotope Biogeochemistry and Natural Denitrification Process in Groundwater: Application to the Chalk Aquifer of Northern France. *Geochim. Cosmochim. Acta* **1988**, *52*, 1869–1878.
(74) McMahon, P. B.; Böhlke, J. K. Regional Patterns in the Isotopic Composition of Natural and Anthropogenic Nitrate in Groundwater, High Plains, U.S.A. *Environ. Sci. Technol.* **2006**, *40* (9), 2965–2970.
(75) Kelepertzis, E.; Matiatos, I.; Botsou, F.; Antonopoulou, C.; Lappas, I.; Dotsika, E.; Chrastný, V.; Boeckx, P.; Karavoltsos, S.; Komárek, M. Assessment of Natural and Anthropogenic Contamination Sources in a Mediterranean Aquifer by Combining Hydrochemical and Stable Isotope Techniques. *Sci. Total Environ.* **2023**, *858* (159763), 1–12.
(76) Burns, D. A.; Kendall, C. Analysis of Δ15N and Δ18O Todifferentiate NO3 Sources in Runoff at Two Watersheds in the CatskillMountains of New York. *Water Resour. Res.* **2002**, *38* (5), 1–11.
(77) Mayer, B.; Bollwerk, S. M.; Mansfeldt, T.; Hütter, B.; Veizer, J. The Oxygen Isotope Composition of Nitrate Generated by Nitrificationin Acid Forest Floors. *Geochim. Cosmochim. Acta* **2001**, *65* (16), 2743–2756.
(78) Spoelstra, J.; Schiff, S. L.; Hazlett, P. W.; Jeffries, D. S.; Semkin, R. G. The Isotopic Composition of Nitrate Produced from Nitrificationin a Hardwood Forest Floor. *Geochim. Cosmochim. Acta* **2007**, *71* (15), 3757–3771.
(79) Romanelli, A.; Soto, D. X.; Matiatos, I.; Martínez, D. E.; Esquius, S. A Biological and Nitrate Isotopic Assessment Framework to Understand Eutrophication in Aquatic Ecosystems. *Sci. Total Environ.* **2020**, *715* (136909), 1–17.
(80) Fang, Y.; Koba, K.; Makabe, A.; Zhu, F.; Fan, S.; Liu, X.; Yoh, M. Low Δ18O Values of Nitrate Produced from Nitrification Intemperate Forest Soils. *Environ. Sci. Technol.* **2012**, *46* (16), 8723–8730.
(81) Snider, D. M.; Spoelstra, J.; Schiff, S. L.; Venkiteswaran, J. J. Stable Oxygen Isotope Ratios of Nitrate Produced from Nitrification: 18 O-Labeled Water Incubations of Agricultural and Temperate Forest Soils. *Environ. Sci. Technol.* **2010**, *44* (14), 5358–5364.
(82) Boshers, D. S.; Granger, J.; Tobias, C. R.; Böhlke, J. K.; Smith, R. L. Constraining the Oxygen Isotopic Composition of Nitrate Produced by Nitrification. *Environ. Sci. Technol.* **2019**, *53* (3), 1206–1216.
(83) Re, V.; Kammoun, S.; Sacchi, E.; Trabelsi, R.; Zouari, K.; Matiatos, I.; Allais, E.; Daniele, S. A Critical Assessment of Widely Used Techniques for Nitrate Source Apportionment in Arid and Semi-Arid Regions. *Sci. Total Environ.* **2021**, *775* (145688), 1–12.
(84) Li, Y.; Yan, W.; Wang, F.; Lv, S.; Li, Q.; Yu, Q. Nitrogen Pollution and Sources in an Aquatic Systemat an Agricultural Coastal Area of Eastern China Based on a Dual-Isotope Approach. *Environ. Sci. Pollut. Res.* **2019**, *26*, 23807–23823.
(85) Nikolenko, O.; Jurado, A.; Borges, A. V.; Knöller, K.; Brouyère, S. Isotopic Composition of Nitrogen Species in Groundwater under Agricultural Areas: A Review. *Sci. Total Environ.* **2018**, *621*, 1415–1432.

Supplementary Material

How the $\delta^{18}O_{NO3}$ versus $\delta^{15}N_{NO3}$ plot can be used to identify a typical expected isotopic range of denitrification for NO_3-impacted groundwaters

Lamine Boumaiza[1], Randy L. Stotler[2], Bernhard Mayer[3], Ioannis Matiatos[4], Elisa Sacchi[5], Neus Otero[6,7], Karen H. Johannesson[8], Frédéric Huneau[9], Romain Chesnaux[10], Mónica Blarasin[11], Viviana Re[12], Kay Knöller[13,14]

[1] University of Texas at Austin, Department of Earth and Planetary Sciences, Jackson School of Geosciences, Austin, Texas, 78712, USA,

[2] University of Waterloo, Department of Earth and Environmental Sciences, Waterloo, Ontario, N2L 3G1, Canada

[3] University of Calgary, Department of Earth, Energy and Environment, Calgary, Alberta, T2N 1N4 Canada

[4] Institute of Marine Biological Resources and Inland Waters, Hellenic Centre for Marine Research, Anavissos Attikis, 19013, Greece

[5] University of Pavia, Department of Earth and Environmental Sciences, Interdepartmental Centre for Water Research, Pavia, 27100, Italy

[6] Universitat de Barcelona, Departament de Mineralogia, Petrologia i Geologia Aplicada, Barcelona, 08028, Spain

[7] Universitat de Barcelona, Institut de Recerca de l'Aigua, Barcelona, 08028, Spain

[8] University of Massachusetts Boston, School for the Environment, Boston, Massachusetts, 02125, USA

[9] Université de Corse, CNRS UMR 6134 SPE, Département d'Hydrogéologie, Corte, 20250, France

[10] Université du Québec à Chicoutimi, Département des Sciences Appliquées, Saguenay, Québec, G7H 2B1, Canada

[11] Universidad Nacional de Río Cuarto, Departamento de Geología, Río Cuarto, Córdoba, X5804BYA, Argentina

[12] University of Pisa, Department of Earth Sciences, Pisa, 56126, Italy

[13] Helmholtz Centre for Environmental Research, Department of Catchment Hydrology, Halle, Saale, 06120, Germany

[14] Technical University of Darmstadt, Institute of Applied Geosciences, Darmstadt, 64287, Germany

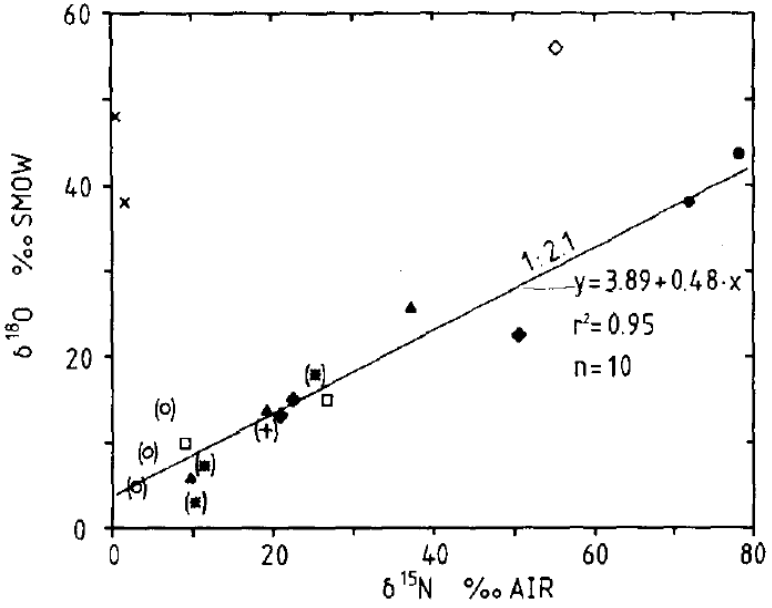
δ18O ‰ SMOW
δ15N ‰ AIR
1:2.1
y=3.89+0.48·x
r²=0.95
n=10

(a)

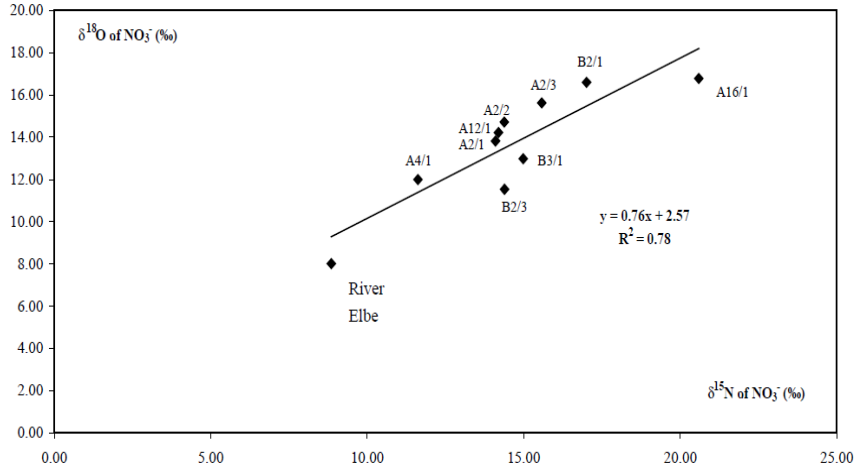
δ18O of NO3- (‰)
δ15N of NO3- (‰)
B2/1
A2/3
A16/1
A2/2
A12/1
A2/1
A4/1
B3/1
B2/3
y = 0.76x + 2.57
R2 = 0.78
River
Elbe

(b)

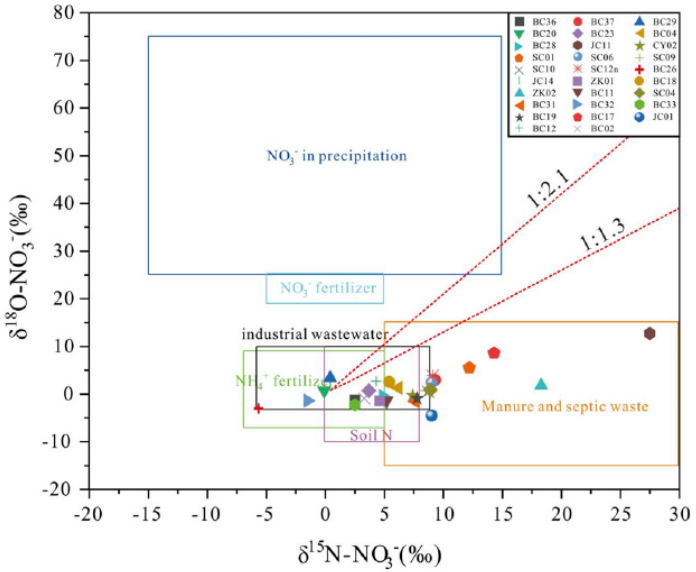
NO3- in precipitation
NO3- fertilizer
industrial wastewater
NH4+ fertilizer
Soil N
Manure and septic waste
1:2.1
1:1.3
δ18O-NO3-(‰)
δ15N-NO3-(‰)

(c)

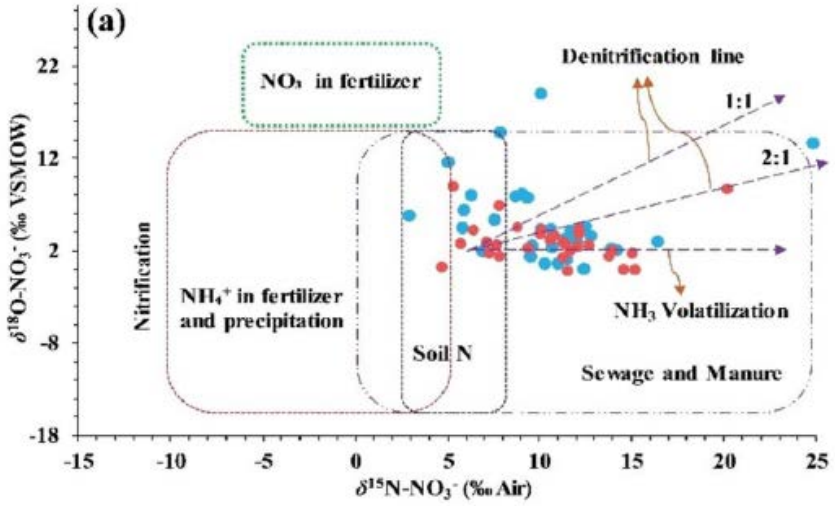
(a)
NOx in fertilizer
Denitrification line
1:1
2:1
Nitrification
NH4+ in fertilizer and precipitation
Soil N
NH3 Volatilization
Sewage and Manure
δ18O-NO3- (‰ VSMOW)
δ15N-NO3- (‰ Air)

(d)

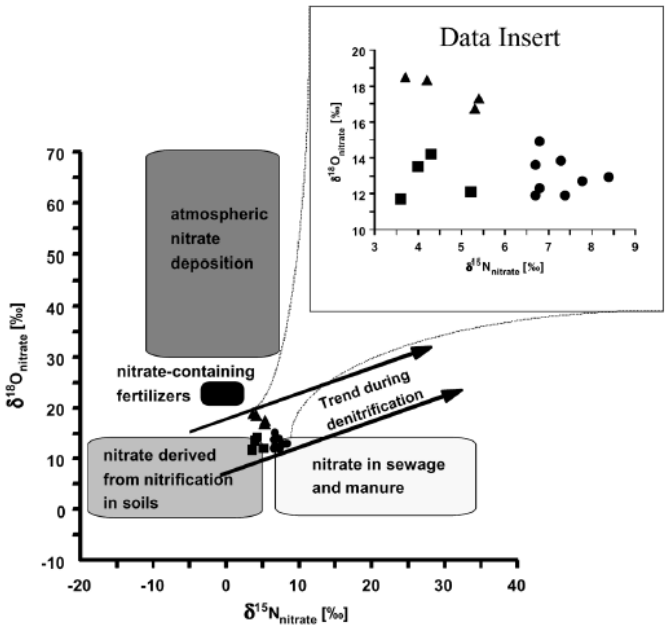
Data Insert
atmospheric nitrate deposition
nitrate-containing fertilizers
Trend during denitrification
nitrate derived from nitrification in soils
nitrate in sewage and manure
δ18O nitrate [‰]
δ15N nitrate [‰]

(e)

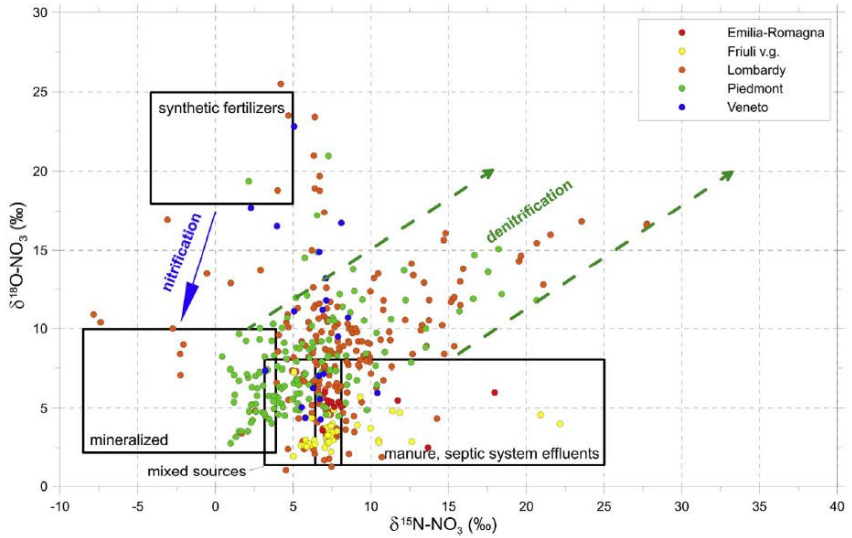
Emilia-Romagna
Friuli v.g.
Lombardy
Piedmont
Veneto
synthetic fertilizers
nitrification
denitrification
mineralized
mixed sources
manure, septic system effluents
δ18O-NO3 (‰)
δ15N-NO3 (‰)

(f)

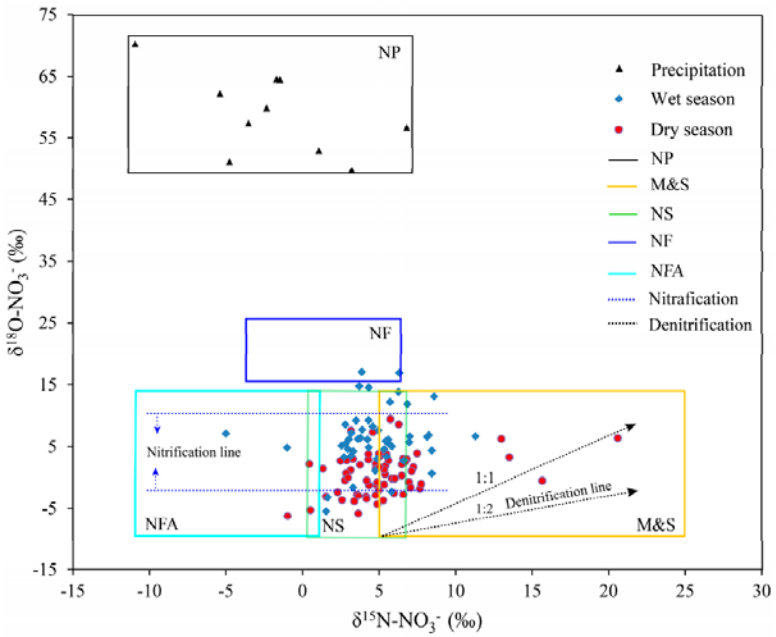
NP
NF
NFA
NS
M&S
Precipitation
Wet season
Dry season
Nitrification
Denitrification
Nitrification line
1:1
1:2
Denitrification line
δ18O-NO3- (‰)
δ15N-NO3- (‰)

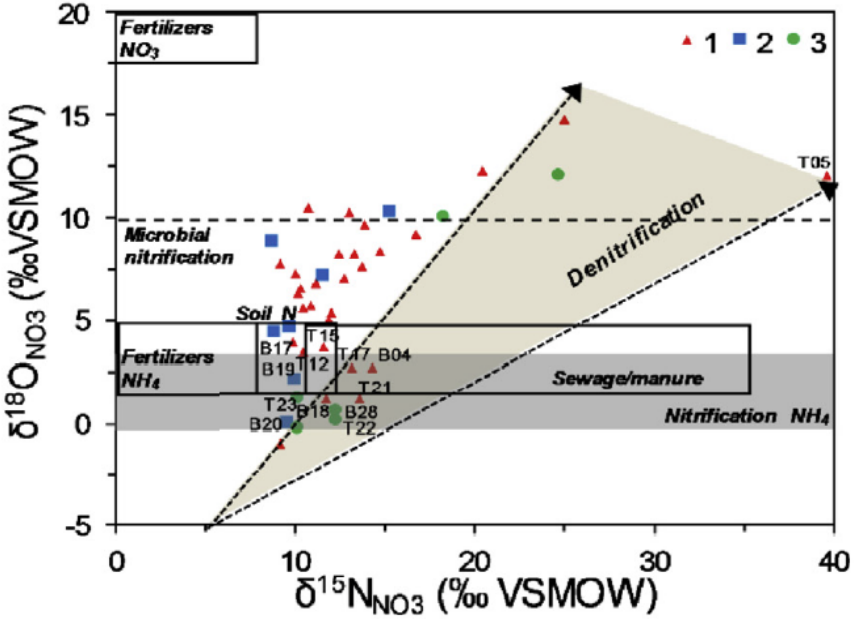
Fertilizers NO3
Microbial nitrification
Soil N
Fertilizers NH4
Sewage/manure
Nitrification NH4
Denitrification
T05
δ18ONO3 (‰VSMOW)
δ15NNO3 (‰ VSMOW)

(g)

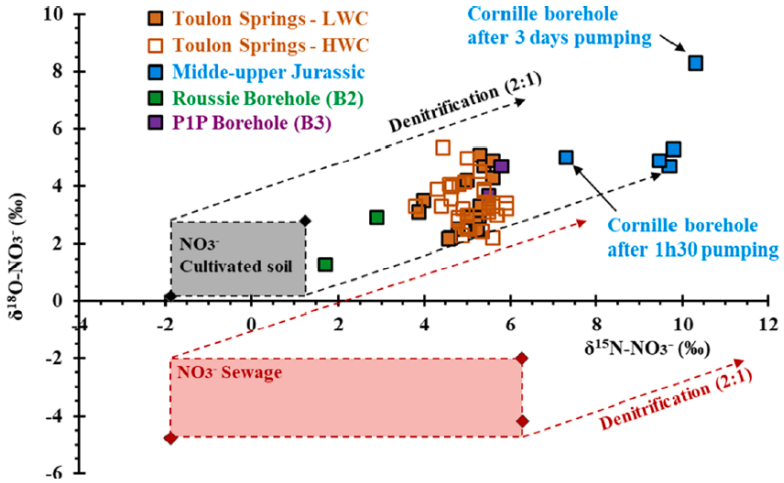
Toulon Springs - LWC
Toulon Springs - HWC
Midde-upper Jurassic
Roussie Borehole (B2)
P1P Borehole (B3)
Cornille borehole after 3 days pumping
Denitrification (2:1)
Cornille borehole after 1h30 pumping
NO3- Cultivated soil
NO3- Sewage
Denitrification (2:1)
δ18O-NO3- (‰)
δ15N-NO3- (‰)

(h)

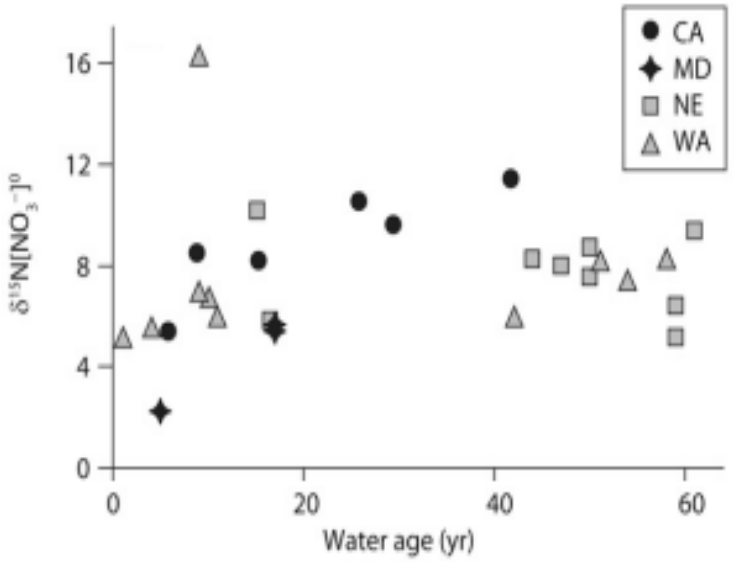
CA
MD
NE
WA
Water age (yr)

(i)

(j)

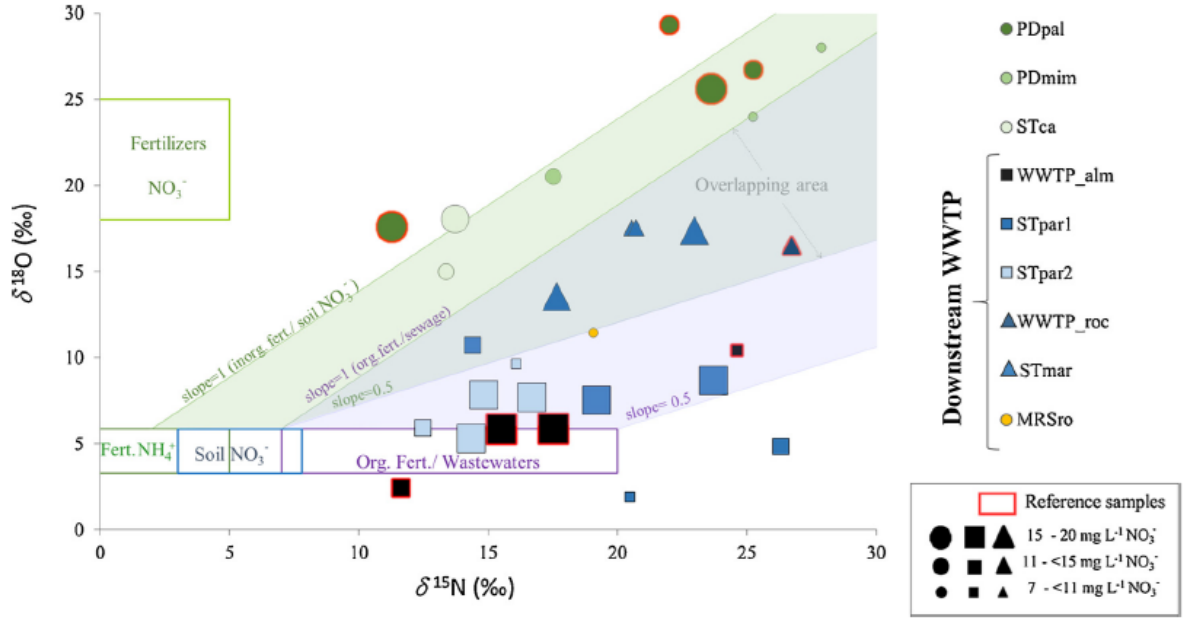
Fertilizers NO3-
Overlapping area
slope=1 (inorg. fert./ soil NO3-)
slope=1 (org.fert./sewage)
slope=0.5
slope= 0.5
Fert. NH4+
Soil NO3-
Org. Fert./ Wastewaters
δ18O (‰)
δ15N (‰)
PDpal
PDmim
STca
Downstream WWTP
WWTP_alm
STpar1
STpar2
WWTP_roc
STmar
MRSro
Reference samples
15 - 20 mg L-1 NO3-
11 - <15 mg L-1 NO3-
7 - <11 mg L-1 NO3-

(k)

Supplementary Figure 1. (a) Determined denitrification line with a slope of 0.48 [1]; (b) Determined denitrification line with slope of 0.76 [2]; (c) Example of $\delta^{18}O_{NO3}$ versus $\delta^{15}N_{NO3}$ plot with the 0.48/0.76-TEIRD from [3]; (d) Example of $\delta^{18}O_{NO3}$ versus $\delta^{15}N_{NO3}$ plot with 0.5/1- TEIRD [4]; (e) Example of TEIRD with two parallel lines [5]; (f) Example of TEIRD with two parallel lines [6]; (g) 0.5/1-TEIRD originating from initial NO_3-isotopic composition corresponding to the lower NO_3-isotope endmembers of manure/sewage field zone [7]; (h) 0.5/1-TEIRD originating from an initial NO_3-isotopic composition having $(\delta^{15}N_{NO3})_0$ value of +5‰ and $(\delta^{18}O_{NO3})_0$ value of −5‰ [8]; (i) Example of TEIRD with two parallel lines originating from same field NO_3 source [9]; (j) Distribution of the reconstructed $(\delta^{15}N_{NO3})_0$ values, using the Böhlke et al. model[10], with groundwater age [11]; (k) Distribution of the measured $\delta^{18}O_{NO3}$ against $\delta^{15}N_{NO3}$ values for samples from Doñana wetland in Spain [12].

Figure 1 (a) is adapted from Böttcher et al [1]. Copyright 1990 with permission of Elsevier; Figure 1(b) is adapted from Fukada et al. [2]. Copyright 2003 with permission of Elsevier; Figure 1 (c) is adapted from Ding et al. [3]. Copyright 2024 with permission of Elsevier; Figure 1 (d) is adapted from Zaryab et al. [4]. Copyright 2024 with permission of Springer Nature; Figure 1 (e) is adapted from Mayer et al. [5]. Copyright 2002 with permission of Springer Nature; Figure 1 (f) is adapted from Martinelli et al. [6]. Copyright 2018 with permission of Elsevier; Figure 1 (g) is adapted from Wang et al. [7] without requiring a permission of the Publisher (no need of permission); Figure 1 (h) is adapted from Torres-Martínez et al. [8] without requiring a permission of the Publisher (no need of permission); Figure 1 (i) is adapted from Lorette et al. [9]. Copyright 2022 with permission of Elsevier; Figure 1 (j) is adapted from Green et al. [11]. Copyright 2008 with permission of John Wiley and Sons; Figure 1 (k) is adapted from Paredes et al. [12]. Copyright 2020 with permission of Elsevier.

Supplementary Table ST1. Data from Heaton et al. [13] for the Stampriel-Auob aquifer in South Africa.

	Measured values	
Sample ID	**NO_3 (mg/L)**	**$\delta^{15}N_{NO3}$ (‰)**
1	55.18	5.1
3	97.34	6.2
4	33.48	17.7
5	21.7	34.9
7	70.68	7.7
43	65.72	5.6
49	50.22	11.2
53	68.82	5.6

Supplementary Table ST2. Data from Boumaiza et al. [14] for the Oussja-Ghar-Melah aquifer in Tunisia, with calculation of % of enrichment.

Sample ID	**Measured value**	**Initial value**	**% of enrichment***
	$(\delta^{18}O_{NO3})$ (‰)	**$(\delta^{18}O_{NO3})_0$ (‰)**	
1	12.9	4.05	69
2	6.1	4.63	25
4	6.0	4.82	20
5	6.7	5.03	25
6	5.7	4.05	30
7	15.6	4.88	69
8	10.1	4.30	57
9	8.9	5.04	44
10	6.5	4.81	26
11	8.9	5.11	43
13	9.1	4.60	49
14	6.5	4.60	29
15	4.7	4.18	11
16	8.4	4.17	50
17	6.4	4.16	34
18	7.9	4.45	43
19	7.7	4.25	44
20	14.8	4.42	70
21	7.3	4.20	42

*: % of enrichment = $[(\delta^{18}O_{NO3}) - (\delta^{18}O_{NO3})_0 \times 100] / (\delta^{18}O_{NO3})$

Supplementary Table ST3. Data from Bourke et al. [15] for agricultural areas CFO1 and CFO4 in Alberta (Canada) – The reconstructed values are not available in Bourke et al. [15] and were provided by the first author (i.e., Bourke, S.).

		Measured values (‰)		Reconstructed values (‰)	
Site	**Sample ID**	$\delta^{15}N_{NO3}$	$\delta^{18}O_{NO3}$	$(\delta^{15}N_{NO3})_0$	$(\delta^{18}O_{NO3})_0$
CFO1	DP11-13_4.3m	30.3	9.8	17.7	0.76
	DP11-13_5.2m	31.0	10.8	20.2	3.06
	DP11-13_7m	31.6	10.2	17.8	0.30
	DP11-13 _7.9m	36.4	14.0	17.5	0.50
	DP11-13_8.8m	29.6	9.9	17.6	1.23
	DC15-22_10m	26.1	7.4	18.1	0.72
	DP10-2	24.2	4.8	17.2	-0.2
	DMW11	33.3	10.9	15.3	-2.0
	DMW12	29.8	14.3	14.7	3.5
	DMW13	23.0	6.8	16.8	2.4
	DP11-12b	35.9	17.0	16.1	2.7
CFO4	BC4	30.6	1.6	20.1	-2.7
	BMW2	41.6	8.3	18.4	-1.2
	BMW5	28.9	6.5	17.3	1.6
	BMW6	70.5	22.1	17.9	0.1
	BMW7	34.0	5.9	17.7	-1.0

Supplementary Table ST4. Data of for $\delta^{15}N_{NO3}$, $\delta^{18}O_{NO3}$ and NO_3 from Otero et al. [16] provided by the first author (i.e., Otero, N.) with the accounted $(\delta^{15}N_{NO3})_0$ and $(\delta^{18}O_{NO3})_0$ values.

Sample ID	$\delta^{15}N_{NO3}$	$\delta^{18}O_{NO3}$	NO_3 (mg/L)	$(\delta^{15}N_{NO3})_0$	$(\delta^{18}O_{NO3})_0$
BAL-001	10.1	1.8	180	3	-2
BAL-005	10.8	3.7	102	5	1
FOL-019	13.8	3.0	141	7	0
GUR-007	13.4	3.8	160	6	0
GUR-101	13.0	2.6	192	5	-1
GUR-106	18.2	4.2	127	12	1
GUR-111	13.4	3.7	124	7	0
GUR-112	12.5	5.6	203	5	2
GUR-113	11.9	2.6	396	3	-2
GUR-115	13.3	5.3	142	6	2
GUR-117	13.5	4.0	302	5	0
GUR-118	14.6	5.2	299	6	1
GUR-119	13.1	4.1	321	4	0
MAL-001	14.8	6.3	118	8	3
MAL-003	13.6	3.8	127	7	1
SCV-003	13.3	4.3	144	6	1
SEB-017	13.2	4.5	156	6	1
TAR-003	12.5	4.2	100	6	1
TON-001	28.3	9.2	18	26	8
TON-002	9.0	0.4	124	2	-3
TON-006	15.6	6.0	102	9	3
TON-007	14.4	5.2	167	7	2
TON-008	18.3	5.2	76	13	2
TAV-003	12.1	2.8	159	5	-1
VIC-004	19.1	7.3	260	11	3
VIC-007	17.9	6.4	100	12	3
VIC-019	14.9	5.0	98	9	2
VIC-100	14.7	5.0	127	8	2
VIC-103	22.2	9.8	17	20	9
BAL-001	9.62	1.13	170	2	-2
BAL-005	9.79	4.49	64	5	2
FOL-019	13.18	3.37	150	6	0
GUR-007	13.27	3.82	204	6	0
GUR-101	13.67	3.51	198	6	0
GUR-106	9.19	1.87	174	2	-2
GUR-111	12.65	3.67	212	5	0
GUR-112	14.40	6.76	170	7	3
GUR-113	11.36	1.81	522	2	-3
GUR-115	13.11	4.88	153	6	1
GUR-117	13.84	3.95	323	5	0
GUR-118	14.11	4.36	286	6	0
GUR-119	12.59	3.68	303	4	0
MAL-001	21.11	10.67	46	17	8
MAL-003	15.10	5.08	151	8	2
SCV-003	13.61	4.53	115	7	1
SEB-017	19.95	8.50	64	15	6
TAR-003	12.19	3.07	278	4	-1
TON-001	10.38	2.96	34.9	6	1
TON-006	15.39	6.01	72	10	3
TON-007	16.57	7.90	123	10	5
TON-008	14.91	3.89	87	9	1
TAV-003	11.98	2.83	203	4	-1
VIC-004	17.72	6.52	333	9	2
VIC-019	13.97	3.80	184	7	0
VIC-100	13.63	3.55	191	6	0
VIC-007	13.06	3.44	98	7	0
VIC-103	18.12	7.08	34.7	14	5
BAL-005	11.2	5.2	153	4	2
GUR-106	10.4	3.6	189	3	0
GUR-111	12.6	6.2	226	5	2
GUR-117	13.6	5.4	390	5	1
GUR-118	14.7	6.5	375	6	2
GUR-119	12.4	5.5	529	3	1
MAL-003	13.5	4.5	164	6	1
TAR-003	12.4	5.0	208	5	1
TON-006	16.0	7.9	99	10	5
TON-008	16.0	6.2	89	10	3
TAV-003	12.3	4.5	256	4	1
VIC-004	16.7	7.1	529	7	2
VIC-007	14.7	5.8	132	8	3
VIC-019	15	6	117	8	3
VIC-103	17.4	9.4	39	13	7
SEB-018	17.11	4.05	10.4	16	3

References

(1) Böttcher, J.; Strebel, O.; Voerkelius, S.; Schmidt, H. L. Using Isotope Fractionation of Nitrate-Nitrogen and Nitrate-Oxygen for Evaluation of Microbial Denitrification in a Sandy Aquifer. *J. Hydrol.* **1990**, *114* (3–4), 413–424.

(2) Fukada, T.; Hiscock, K. M.; Dennis, P. F.; Grischek, T. A Dual Isotope Approach to Identify Denitrification in Groundwater at a River-Bank Infiltration Site. *Water Res.* **2003**, *37* (13), 3070–3078.

(3) Ding, K.; Zhang, Y.; Zhang, H.; Yu, C.; Li, X.; Zhang, M.; Zhang, Z.; Yang, Y. Tracing Nitrate Origins and Transformation Processes in Groundwater of the Hohhot Basin's Piedmont Strong Runoff Zone through Dual Isotopes and Hydro-Chemical Analysis. *Sci. Total Environ.* **2024**, *919* (170799), 1–17.

(4) Zaryab, A.; Alijani, F.; Knoeller, K.; Minet, E.; Musavi, S. F.; Ostadhashemi, Z. Identification of Groundwater Nitrate Sources in an Urban Aquifer (Alborz Province, Iran) Using a Multi-parameter Approach. *Environ. Geochem. Health* **2024**, *46* (100), 1–17.

(5) Mayer, B.; Boyer, E. W.; Goodale, C.; Jaworski, N. A.; Van Breemen, N.; Howarth, R. W.; Seitzinger, S.; Billen, G.; Lajtha, K.; Nadelhoffer, K.; Van Dam, D.; Hetling, L. J.; Nosal, M.; Paustian, K. Sources of Nitrate in Rivers Draining Sixteen Watersheds in the Northeastern U.S.: Isotopic Constraints. *Biogeochemistry* **2002**, *57* (58), 171–197.

(6) Martinelli, G.; Dadomo, A.; De Luca, D. A.; Mazzola, M.; Lasagna, M.; Pennisi, M.; Pilla, G.; Sacchi, E.; Saccon, P. Nitrate Sources, Accumulation and Reduction in Groundwater from Northern Italy: Insights Provided by a Nitrate and Boron Isotopic Database. *Appl. Geochemistry* **2018**, *91*, 23–35.

(7) Wang, M.; Lu, B.; Wang, J.; Zhang, H.; Guo, L.; Lin, H. Using Dual Isotopes and a Bayesian Isotope Mixing Model to Evaluate Nitrate Sources of Surface Water in a Drinking Water Source Watershed, East China. *Water* **2016**, *8* (355), 1–16.

(8) Torres-Martínez, J. A.; Mora, A.; Mahlknecht, J.; Daessle, L. W.; Cervantes-Aviles, P. A.; Ledesma-Ruiz, R. Estimation of Nitrate Pollution Sources and Transformations in Groundwater of an Intensive Livestock-Agricultural Area (Comarca Lagunera), Combining Major Ions, Stable Isotopes and MixSIAR Model. *Environ. Pollut.* **2021**, *269* (115445), 1–12.

(9) Lorette, G.; Sebilo, M.; Buquet, D.; Lastennet, R.; Denis, A.; Peyraube, N.; Charriere, V.; Studer, J. C. Tracing Sources and Fate of Nitrate in Multilayered Karstic Hydrogeological Catchments Using Natural Stable Isotopic Composition (Δ15N-NO3 and Δ18O-NO3). Application to the Toulon Karst System (Dordogne, France). *J. Hydrol.* **2022**, *610* (127972), 1–14.

(10) Böhlke, J. K.; Wanty, R.; Tuttle, M.; Delin, G.; Landon, M. Denitrification in the Recharge Area and Discharge Area of a Transient Agricultural Nitrate Plume in a Glacial Outwash Sand Aquifer, Minnesota. *Water Resour. Res.* **2002**, *38* (7), 1–25.

(11) Green, C. T.; Puckett, L. J.; Böhlke, J. K.; Bekins, B. A.; Phillips, S. P.; Kauffman, L. J.; Denver, J. M.; Johnson, H. M. Limited Occurrence of Denitrifi Cation in Four Shallow Aquifers in Agricultural Areas of the United States. *J. Environ. Qual.* **2008**, *37* (3), 994–1009.

(12) Paredes, I.; Otero, N.; Soler, A.; Green, A. J.; Soto, D. X. Agricultural and Urban Delivered Nitrate Pollution Input to Mediterranean Temporary Freshwaters. *Agric. Ecosyst. Environ.* **2020**, *294* (106859), 1–12.

(13) Heaton, T. H. E.; Talma, A. S.; Vogle, J. C. Origin and History of Nitrate in Confined Groundwater in the Western Kalahari. *J. Hydrol.* **1983**, *62*, 243–262.

(14) Boumaiza, L.; Ben-Ammar, S.; Chesnaux, R.; Stotler, R. L.; Mayer, B.; Huneau, F.; Johannesson, K. H.; Levison, J.; Knöller, K.; Stumpp, C. Nitrate Sources and Transformation Processes in Groundwater of a Coastal Area Experiencing Various Environmental Stressors. *J. Environ. Manage.* **2023**, *345* (118803), 1–11.

(15) Bourke, S. A.; Iwanyshyn, M.; Kohn, J.; Hendry, M. J. Sources and Fate of Nitrate in Groundwater at Agricultural Operations Overlying Glacial Sediments. *Hydrol. Earth Syst. Sci.* **2019**, *23*, 1355–1373.
(16) Otero, N.; Torrento, C.; Soler, A.; Mencio, A.; Mas-Pla, J. Monitoring Groundwater Nitrate Attenuation in a Regional System Coupling Hydrogeology with Multi-Isotopic Methods: The Case of Plana de Vic (Osona, Spain). *Agric. Ecosyst. Environ.* **2009**, *133*, 103–113.